Asian Journal of Chemistry; Vol. 34, No. 6 (2022), 1313-1332

ASIAN JOURNAL OF CHEMISTRY

https://doi.org/10.14233/ajchem.2022.23716

REVIEW

Super Material Borophene: Next Generation of Graphene

KESHAV DEV[1], ANKIT K SRIVASTAVA[2], SWASTI SAXENA[3,*], B.S. BHADORIA[4] and BARISH DWIVEDI[1]

[1]Department of Physics, Raghuveer Singh Government Degree College, Lalitpur-284403, India
[2]School of Science, Indrashil University, Mehsana, Gandhinagar-382740, India
[3]Department of Physics, Sardar Vallabhbhai National Institute of Technology, Surat-395007, India
[4]Department of Physics, Bundelkhand University, Jhansi-284003, India

*Corresponding author: E-mail: swastisaxenaa@gmail.com

Received: 6 January 2021; *Accepted*: 20 February 2022; *Published online*: 18 May 2022; AJC-20789

In this review article, we discussed about how the new wonder material borophene is stronger and more flexible than graphene. It's an excellent conductor of both electricity and heat, as well as a one-of-a-kind superconductor. The orientation of the material and the arrangement of vacancies affect these properties. Borophene is also rather light and reactive. Graphene is the wonderful material not long ago. Tubes, balls and other strange shapes can be formed from a super-strong, atom-thick sheet of carbon. The idea of a new age of graphene-based computer processing and a rich graphene chip industry has been highlighted by materials scientists. However, the remarkable qualities of borophene have lately astonished everyone. It has optimum strength and in-plane flexibility. In some combinations, they can be stronger and more flexible than graphene. Borophene's high theoretical specific capacities, electrical conductivity and ion transport capabilities make it a promising anode material for batteries. Borophene has a wide range of possible applications due to its unusual physical and chemical features. It is capable of accelerating the decomposition of hydrogen and oxygen, is light weight and can acts as a reactant. We describe the work on borophene in this review, with a focus on current developments. The phases of borophene are first introduced through experimental synthesis and theoretical predictions. The physical and chemical qualities are then summarized, including mechanical, thermal, electrical, optical and superconducting properties.

Keywords: Borophene, Graphene, Properties, Synthesis.

INTRODUCTION

Graphene is the first two-dimensional substance identified [1]. The remarkable features of graphene have given rise to a new class of materials known as "2D materials" [2-5]. For many applications, 2D forms are a relatively fascinating and fresh topic [6]. 2D materials often offer a variety of physical features that make them attractive for electronic devices, photonics, energy conversion and nanoengineering [7-10]. 2D materials such as phosphorene, boron nitride, germanene, antimonene, silicene, arsenene and transition metal dichalcogenides have recently attracted a lot of attention due to the rapid growth of graphene. The mass of atom-thick materials has been predicted or produced theoretically [11-15]. Surprisingly, due of the various out-of-plane buckling degrees, they have distinct structures than graphene [16]. Some 2D materials, such as the combination of 2D flat boron, 2D gallium nitride (GaN) and hafenene [17], may be created from bulk materials without layered form in addition to exfoliated 2D materials from their layered bulk counterparts.

Graphene is regarded as a miraculous substance. It is made out of a one-atom thick sheet of carbon that is extremely strong, conducts electricity and can be shaped into any shape. The European Union has put one billion Euros towards launching a graphene sector and the material has been utilized in everything from apparel to condoms to paint. So, what is it about graphene that makes us want to mass-produce it so badly? Graphene is known as a "wonder material" for a reason: it possesses a number of exceptional features that scientists have linked to a variety of possible uses [18,19]. It's thin and flexible,

but it's also stronger than diamond and it's one of the strongest materials known, with strength of roughly 200 times stronger than steel. This is despite the fact that it is extremely thin and light, weighing just 0.77 mg/m^2. It is also a better conductor of electricity and heat than copper. It may be coiled into balls, rolled into tubes, or piled to produce graphite once again.

Graphene's position as a "wonder substance" is being questioned more than a decade after its discovery. Not everyone believes that a 'killer' application would ever offset the expenditures of its development. The total expenditure in graphene research is now expected to be US $ 2.4 billion; yet, only US $ 12 million worth of graphene was sold in 2013. Many have referred to carbon nanotubes, which had a slew of potential applications when they were discovered, but failed to live up to much of the hype. While graphene hasn't yet realized its full potential, there's still time and with the amount of current research being done, it's certainly feasible.

Hexagonal boron-nitride, graphitic carbon nitride, silicene and germanene, as well as dichalcogenides like molybdenum disulfide, all follow graphene in close succession. Borophene is one of the most recent breakthroughs. It is the most recent substance to challenge graphene's claim to the kingdom. One layer of boron atoms forms numerous crystalline shapes in this material. Borophene is a relatively new compound. The material was initially predicted using computer models in the 1990s, but it wasn't synthesized until 2015 *via* chemical vapour deposition. A heated gas of boron atoms condenses over a cold surface of pure silver in this procedure. Researchers from MIT, USA and Xiamen University in China have discovered a slew of unexpected properties in borophene, a two-dimensional material with the potential to outperform graphene. Borophene is made up of the same boron and carbon components as graphene. This is critical because, despite their macroscopic allotropes being quite different, small atomic clusters of carbon and boron are quite similar at the nanoscale. Prior to the discovery of graphene, the presence of a 2D boron substance like it was predicted theoretically [20-23].

The genuine material was created using the molecular beam epitaxial growth method. That is, elemental boron was deposited on a silver surface under extreme vacuum. To begin with, borophene is stronger and more flexible than graphene, which is an important attribute when considering that graphene is harder than diamond and is made entirely of carbon (one of the hardest elements that exist on the planet). Borophene is also an electrical superconductor. Its unique crystalline structure, which is created by boron atoms, is responsible for this property, since the gaps that remain between the atoms allow boron to be superconducting [24].

Borophene's capacity to catalyze the decomposition of hydrogen and oxygen is one of its most notable advantages. It has excellent catalytic effects in the hydrogen evolution process, oxygen reduction reaction, oxygen evolution reaction and CO_2 electro-reduction reaction [25]. This might usher in a new age of water-based energy generation. However, scientists must complete a significant amount of research before borophene usage may be considered a possibility. Given that borophene's reactivity renders it susceptible to oxidation, there is still a long way to go in terms of finding a technique to generate significant amounts of the material. These two factors make borophene difficult to handle and expensive to manufacture, just like graphene.

Both materials are closely related and their atomic structures are so similar (Fig. 1). The systematic arrangement of silver atoms drives boron atoms into a similar pattern, with each atom forming a flat hexagonal shape by connecting to as many as six other atoms. However, a large number of boron atoms connect with just four or five other atoms, resulting in voids in the structure. The pattern of vacancies in borophene crystals is what gives them their distinct features. It turns out that borophene is both stronger and more flexible than graphene. It also superconducts and is an excellent conductor of both electricity and heat. The characteristics of the material vary based on its orientation and the arrangement of vacancies, indicating that it is 'tunable.' Furthermore, borophene has the potential to be used in batteries and as a hydrogen production catalyst. Other issues with graphene include its mechanical rigidity, which makes it unsuitable for systems that require extensive compression, stretching or torsion tolerance. It has

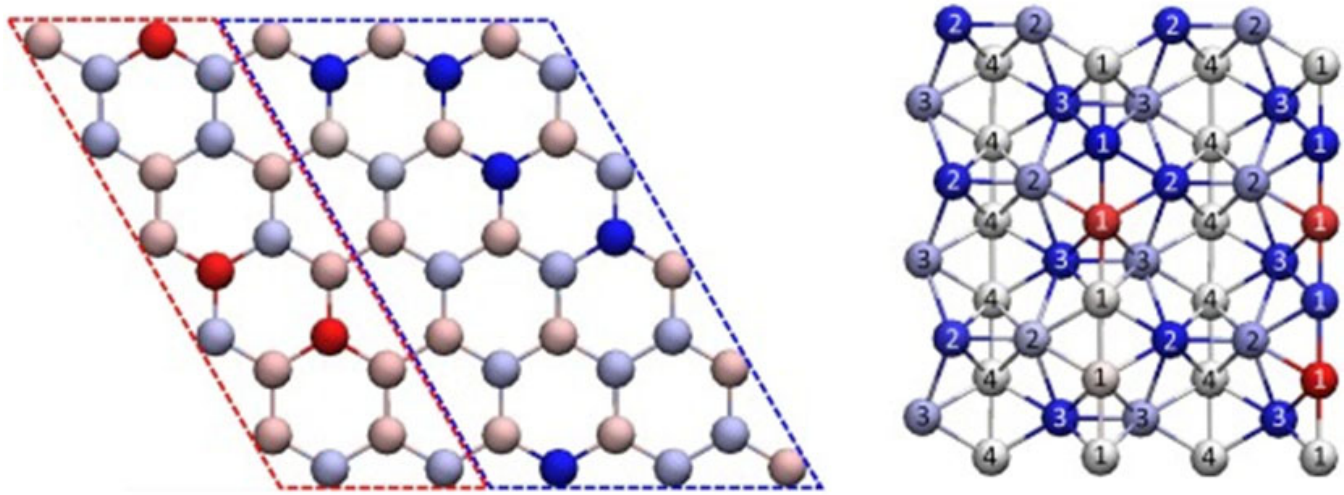

(a) Graphene structure (b) Borophene structure

Fig. 1. Structure of (a) graphene, (b) borophene

a band-gap that makes it unsuitable for simple on/off switching. Because of its oxidation susceptibility, it cannot be employed as a catalyst in oxidizing settings. Furthermore, it may contain sharp edges that might rip cell membranes and cause them to malfunction. The trouble with graphene is that it lacks one of these bandgaps. This implies that electrons can flow through it at any energy; it can't be turned off. While scientists have attempted to artificially produce a band-gap in graphene with little success, this is an important function for transistors. Many scientists have now put their hopes for silicon replacement on other 2D materials with a band-gap, which have been found since graphene.

The biggest impediment to 'the era of borophene' is that it is now impossible to manufacture in significant numbers. Furthermore, the material is prone to oxidation. Regardless, borophene has a lot of promises and might be the next graphene. It was recently synthesized using molecular beam epitaxy and now researchers from Rice University in the United States and Nanjing University of Aeronautics and Astronautics in China report their complete first-principles analyses of the mechanical properties of borophene in advanced functional materials.

Although borophene is comparable to graphene in terms of its lightness and strength, it has two distinct characteristics that lead to its unexpected attractive attributes. First, borophene is made up of a highly changeable boron atom network of hollow hexagons in a reference triangular lattice and its mechanical characteristics may be tailored by varying the hollow hexagon concentration (Fig. 2). Second, due to its delocalized multi-centered bonding, borophene is metallic in nature, which the researchers believe might predict qualitatively novel behaviours.

The researchers discovered that borophene possesses "record high" flexibility, a better stiffness to weight ratio than graphene and a higher ideal strength than the most well-known polymer materials in this study. Rather of shattering under strain like many other materials, borophene undergoes strain-induced structural phase changes, which further reinforce the material. Furthermore, by adding more hollow hexagons to the network, its material strength is increased, allowing us to adjust and fine-tune the material features.

The substance graphene has captivated the scientific community for years due to its amazing strength and flexibility. At room temperature, it conducts electricity better than any other substance. It was designed to hold electrical data and has the potential to change the way we create computer chips. Our best contender for constructing in space is a 3D variant of graphene. People have speculated about whether the material will spark the next industrial revolution. It's even put it into commercial goods like light bulbs and coats and graphene hair dye might be next.

This brave new graphene-based future is still a long way off. However, it has sparked curiosity about alternative 2D materials. The most interesting of them is borophene, which is made up of a single layer of boron atoms that may create a variety of crystalline forms. Since the production of 2D boron sheets (borophene) on silver substrates in 2015. In the domains of condensed matter physics, chemistry, material science and nanotechnology, research on borophene has exploded.A variety of applications of borophene for example, alkali metal ion batteries, Li-S batteries, hydrogen storage, supercapacitor, sensor and catalytic in hydrogen evolution, oxygen reduction,

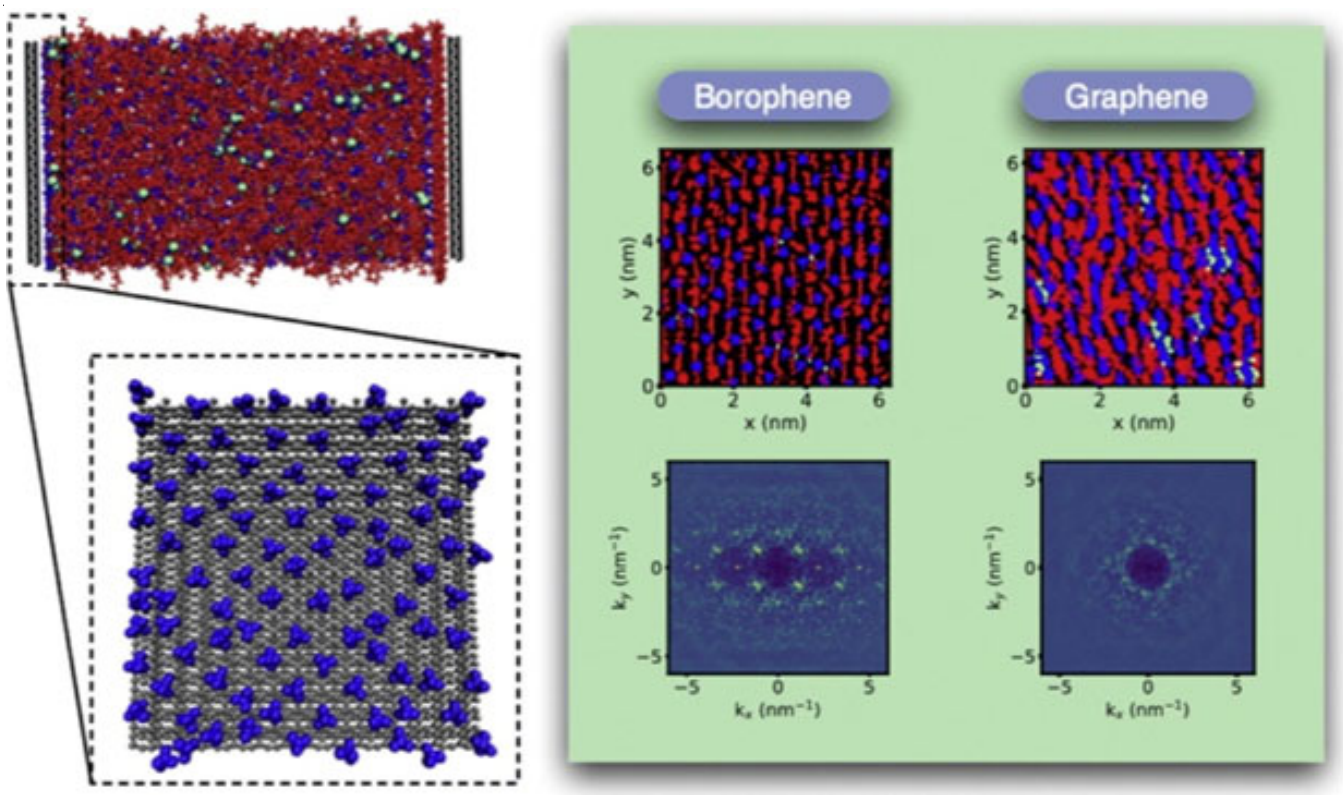

Fig. 2. Surface morphology of graphene and borophene

oxygen evolution and CO_2 electroreduction reaction [26,27] are also reported. It can store more than 15% of its weight in hydrogen. Finally, based on its current state of development, the obstacles and prospects in this potential sector are highlighted.

Because boron has the unusual ability of combining with practically all other elements, study on boron in diverse compounds may be dated back several hundred years. Hexagonal boron nitride (h-BN) is a large band-gap III-V compound among them. It's a graphite-like layered material with planar networks of h-BN hexagons stacked in a regular pattern. The chemical stability, physical characteristics and thermal conductivity of h-BN are all outstanding [28-30]. Because it is so similar to graphite, it is possible to make pure boron from it. Kolmogorov & Curtarolo *et al*. [31] were the first to document pure boron in 1957, as well as the bulk g-B106 with an extraordinarily complex structure. Bulk boron is known to contain more than 16 polymorphs, all of which have interconnected polyhedral structure but only a handful of which have a crystal structure.

In 2015, argentum (Ag) substrates were successfully used to construct a 2D boron sheet [32]. Many researchers from many domains, including material science, nanotechnology, physics, chemistry and condensed matter, have been drawn to the study of borophene [33-35]. "Borophene" is a novel atom-thick boron nanosheet that might be used in large-scale synthesis [36]. To date, it is the lightest 2D substance. Borophene is a close relative of graphene, thus it is hoped that it will have some of the same characteristics as graphene [37]. The electronic states of the Fermi-surface are occupied by both and electrons in borophene, making it superconductive. Due to the lack of external strain or pressure, borophene may have the highest tensile strength of any 2D material. The chemical and structural complexity, electrical characteristics and stability of 2D boron structures have all been widely explored [38-41].

The mechanical qualities of borophene are extremely intriguing and crucial. To begin with, borophene has a very low mass density. Borophene can be utilized as an assist element in composite construction if its ideal strength and in-plane stiffness are satisfactory. Second, because of its great flexibility against off-plane deformation, borophene is useful for constructing flexible [42,43] nanodevices. Furthermore, borophene's magnetic and electrical characteristics may be efficiently tuned for a variety of applications due to its strongly anisotropic structure [44,45]. Borophene is polymorphic, which distinguishes it from other 2D materials [46] due to the abundance of bonding orientations among the boron atoms. Within the range of 10-20 K, boron's low mass density induces significant electron-phonon coupling, resulting in phonon-mediated superconductivity with a high critical temperature [47,48]. In a nut-shell, borophene is abundant in resources, has a low atomic weight, is light, cheap and has great electrical properties. Because of these benefits, borophene will have more practical applications in the future.

Despite the various potential uses of borophene, the synthesis and finding of its neoatomic structures with well-designed structure-property interactions remains one of the most difficult tasks. Furthermore, for synthetic 2D materials, many parameters such as component elements, processing conditions and growth substrates impact the resultant atomic structure (Fig. 3). The synthesis of high-quality specimens and the separation of borophenes from substrates remain difficult to achieve in practise, necessitating ongoing experimental and theoretical efforts [17].

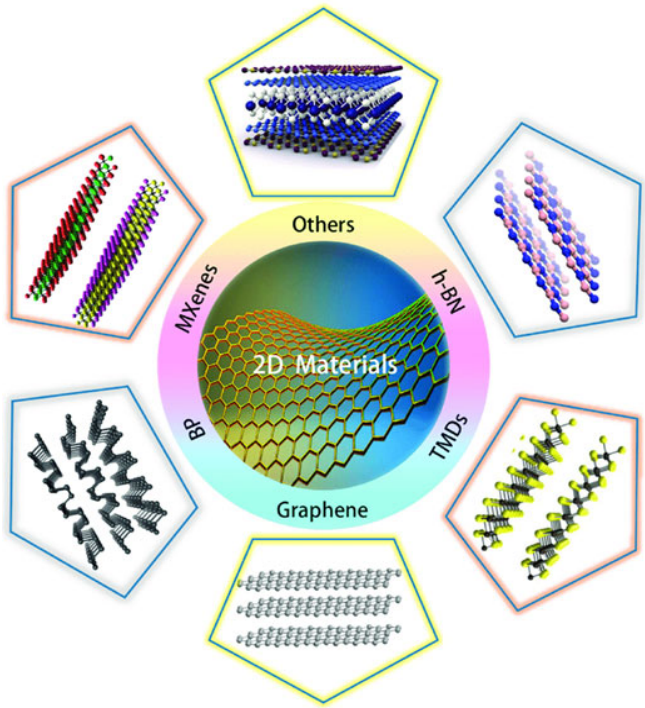

Fig. 3. 2-Dimentional materials

Graphene *vs.* borophene properties

Graphene

Electronic structure: Because of its crystal structure, graphene has an unique band structure. On a two-dimensional plane, carbon atoms form a hexagonal lattice. Each carbon atom is about a =1.42 Å away from its three neighbours, with whom it shares one bond. A-bond, which is orientated in the *z*-direction, is the fourth bond (out of the plane). The orbital can be seen as a pair of symmetric lobes aligned along the *z*-axis and centred on the nucleus. Each atom has one of these π-bonds, which are then hybridized to produce the π-band and π^*-bands. The majority of graphene's unusual electrical characteristics are due to these bands. Graphene's hexagonal lattice is made up of two interlocking triangular lattices. Fig. 4 shows how this works.

Graphene has become a fascinating substance that has piqued the curiosity of scientists. In the realm of condensed matter physics, monolayer graphene sparked a renewed interest in 2D materials [49]. Based on its interesting qualities, graphene has motivated many scientists to create a new future in the fields of electronic, magnetic and photonic research [2-4]. Graphene has amazing electrical properties due to its high electron mobility at ambient temperature. Transition metal chalcogenide (TMDs) are being researched to use their exceptional electronic and magnetic properties [50]. Graphene is an atomically thick 2D material and transition metal chalcogenide

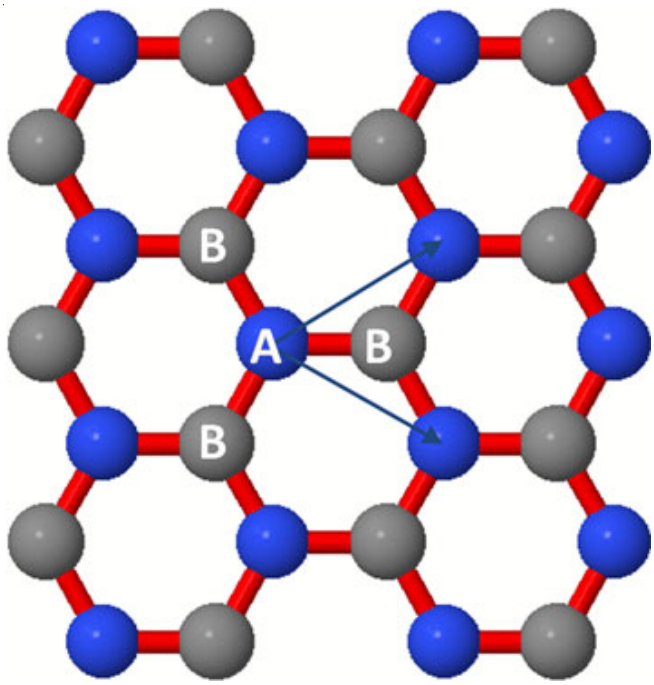

Fig. 4. Electronic structure of boron

are being studied with great effort to use their exceptional electronic and magnetic properties. Graphene, a one-atom-thick sheet of carbon atoms, exhibits a number of unique features [4], including enormous intrinsic mobility, zero effective mass, extremely high thermal conductivity [5,6,51], stiffness and magnetic and optical properties.

Dirac fermions: In Fig. 5, the cone-like linear dispersion relation can be seen at one of the graphene Dirac points. For neutral (or perfect) graphene, the Fermi energy is equal to the Dirac energy, which is the energy of the Dirac point. The Fermi energy in graphene devices can deviate greatly from the Dirac energy. A linear dispersion relation exists for electrons within roughly 1 eV of Dirac energy. The Dirac equation for massless

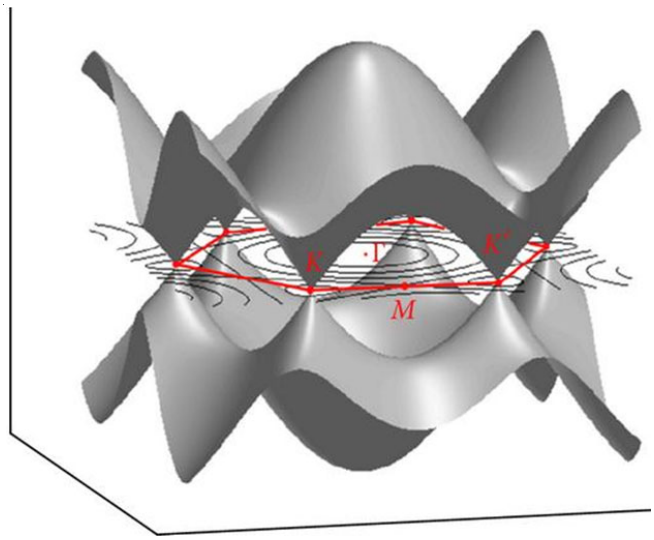

Fig. 5. First Brillouin zone and band structure of graphene. The vertical axis is energy, while the horizontal axes are momentum space on the graphene lattice. The Dirac points are the transition between the valence band and the conduction band

fermions accurately describes the linear dispersion area. That is, the charge carriers' effective mass in this area is zero. Charge carriers in graphene act like relativistic particles with a Fermi velocity, which determines their effective speed of light. This behaviour is one of the most fascinating properties of graphene and it is responsible for most of the graphene research interest [52].

Chirality: Many researchers reported the chirality of graphene transport in a bit more detail later. Each graphene sublattice is responsible for a different branch of the dispersion. These dispersion branches have relatively little interaction with one another. This chiral effect suggests that the charge carriers have a pseudospin quantum number. This quantum number is similar to spin, although it is unrelated to the "actual" spin. The pseudospin allows researchers to distinguish contributions from each sublattice. Because one type of dispersion cannot be transformed into another, this independence is known as chirality [53,54]. Researchers couldn't turn a right hand into a left hand using simply translations, scalings and rotations, as an illustration of chirality. The Pauli matrix contributions in the Dirac-like Hamiltonian discussed in the preceding section may also be used to explain graphene chirality.

Vibrational properties: While the electrical characteristics of graphene have sparked the most interest, the vibrational properties are as important [55,56]. They are responsible for a number of intriguing features, including high thermal conductivities. Because graphene is made up of light atoms with extremely strong inplane bonding, it has a very fast sound velocity. The high heat conductivity of graphene, which is advantageous in many applications, is due to its enormous sound velocity. Furthermore, vibrational characteristics are important for understanding other graphene features, including as optical properties (*e.g.*, Raman scattering) and electrical properties (electron-phonon scattering).

Phonon dispersion: The phonon dispersion relation may be used to understand most of graphene's vibrational characteristics. Surprisingly, the phonon dispersion resembles the electrical band structure in certain ways. The vibrational modes of the crystal in thermal equilibrium must be considered in order to determine the phonon dispersion. This is done by looking at how much each atom has moved away from its equilibrium point. Some torsional and longitudinal force constants, which simply rely on the relative locations of the atoms, efficiently connect each atom to its neighbours.

Neutron scattering, electron energy loss spectroscopy, X-ray scattering, infrared absorption and double resonant Raman scattering experiments were used to get the findings [57]. Although there is no comparable amount of data on graphene, it is believed to be quite similar to graphite because to the poor connection between planes. The majority of graphene data comes from Raman scattering, which allows the phonon spectrum to be determined at certain symmetry points.

Physical and chemical properties: Despite graphene's extraordinary physical and chemical capabilities [58], the lack of a large band-gap has slowed the development of graphene based electrical and photonic research and technology. A number of research groups have attempted to open a band-gap in

graphene by using one of two methods: (1) creating graphene nanoribbons [59,60] with a few nanometres in width or (2) chemical alteration of the graphene surface. The graphene nanoribbon has shown the capacity to tune the band-gap by a factor of ten and switchable nano-devices. Ribbon widths of the order of a nanometre are difficult to manage. Chemical approaches, on the other hand, are more viable for large-scale manufactures and industrial uses. 2D materials have a wide range of applications in electronic devices, energy storage and utilization due to their unique physical and chemical features (such as linear band structure around the Fermi level, high electrical and thermal conductivity and stiffness).

Borophene

Electronic structure borophene: Since boron is positioned between non-metallic carbon and metallic beryllium, contains only three valence electrons [$2s^2 2p^1$]. The orbit radius of the 2*p* electron is close to that of the 2*s* state, giving it both metallicity and non-metallicity. The unique electronic structure of bulk boron allows for the development of a wide range of bonding and enables the production of remarkable bonds. When compared to other 2D materials, 2D boron gives more energy alleviation [1,2,17,24]. The most stable form for the electron-deficient B element is a combination of hexagonal and triangular structures with two and three centre bonding, respectively [61-63]. Despite its differences from graphene's stable structure, borophene possesses certain unusual electrical characteristics, including metallicity, Dirac-Fermi effects, superconductivity and semiconductivity.

Dirac point at borophene: Dirac materials are no longer restricted to carbon-based materials; they now encompass a wide range of other materials too [52]. Boron, being the left side light element of carbon atom, has a lot of promise for spawning 2D Dirac materials that are comparable to carbon materials in many ways. The findings point to monolayer boron as a potential material for high-speed, low-dissipation nanodevices.

Since it was successfully synthesized on silver, the topological features of 12 borophene have been a focus (111). Feng *et al.* [64] used first principles calculations to prove that 12 borophene had Dirac fermions, confirming the first non-honeycomb monolayer Dirac material. The bands at the Fermi level of 12 borophene have been found to be separated from the p_z orbit, similar to graphene. Furthermore, using a basic tight-binding model and just considering the p_z orbit on the free-standing 12 borophene, the Dirac cones were discovered at ($\pm 2\pi/3a$, 0) of the first Brillouin zone (BZ) in the freestanding 12 borophene. 12 borophene may be dissolved into two triangular sublattices and therefore host Dirac cones, similar to the honeycomb lattice and the splitting of the Dirac cones is governed by sublattice symmetry (Fig. 6). Meanwhile, Meng *et al.* [65] claimed that using periodic perturbations, each Dirac cone may be divided and the split Dirac cones are nonconcentric, unlike graphene. Researchers have explored the origin of Dirac fermions in β12 on Ag(III) and freestanding β12 borophene, respectively.

Wang *et al.* [66] used an *ab initio* evolutionary structure search approach to propose a new type of borophene, *P*mmn borophene with massless Dirac fermions and twisted Dirac cone [21,67,68]. *P*mmn is the third metal Dirac material and the first 2D Dirac boron material, with a graphene-like plane and B2 pairs, between which there is a strong charge transfer and massless double Dirac cones with a higher Fermi velocity than graphene, increasing the energy stability of *P*6/mmm borophene [21,69].

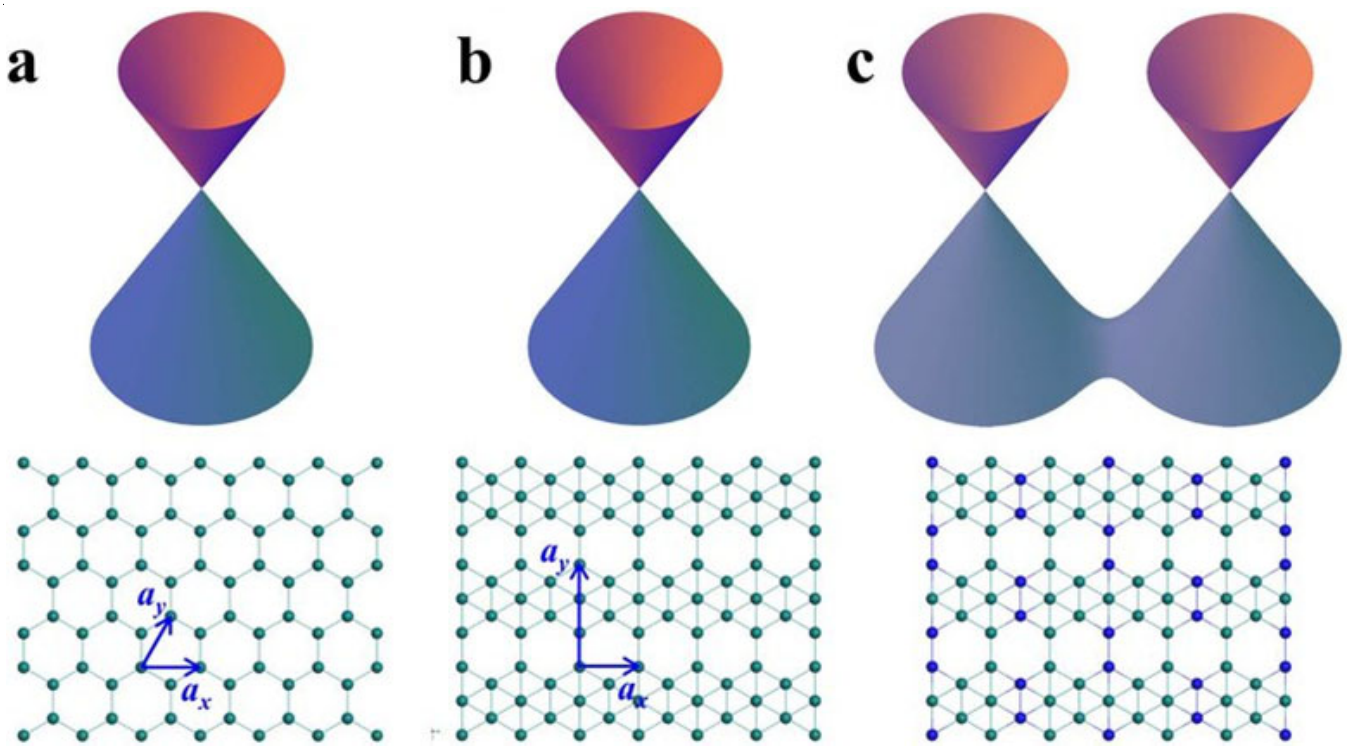

Fig. 6. 2D Dirac boron

Chirality: Because this borophene phase contains two chiral variations, the stacking sequence may be designed. It is shown that an external electric field may affect the orbital texturing and layer localization by combining the orbital pseudospin with this layer degree of freedom. The orbital texture of the same chirality stacking is particularly resistant to the electric field. The electric field, on the other hand, permits an on/off switch of the orbital-pseudospin Dirac cone for stackings of layers with opposing chirality [70].

Mechanical properties: Borophene offers outstanding mechanical characteristics since it is made up of multicenter covalent connections rather than the traditional two-center covalent bonds found in other 2D materials [71-73], which has a bond energy of 5.90 eV. In case of the borophene, metallic like multicenter linkages supply the structure with potential fluidity in addition to the traditional covalent bonds that give the sheet its strength [74]. The flat construction eliminates the instability produced by the triangular boron sheet's buckling structure. As previously stated, the insertion of hollow hexagons into borophene can effectively stabilize the structure because the applied strain is significantly concentrated at hollow hexagons, controlling the elasticity of the whole sheet [75]. Hollow hexagons, on the other hand, can extend the sheet area, lowering tension and the structural phase change experienced by borophene can make the material harder and resist huge loads even in great tension. Hence, hollow hexagons are crucial for the ductile breaking process of borophene. Hollow hexagons, on the other hand, have a significant impact on the mechanical characteristics of materials. Increasing the number of hollow hexagons reduces the amount of B–B bonds and hence the material's hardness. The boron lattice's final tensile strength will likewise be considerably influenced. In other words, despite the increase in, the changes in borophene stifness are restricted by just adding hollow hexagons. As a result, these mechanical qualities may be changed as needed to satisfy the requirements of different applications. The failure mechanism of borophene was also investigated [17], revealing that under a uniaxial strain along the zigzag direction, the failure mechanism is elastic instability, whereas under a uniaxial strain along the armchair direction and biaxial strain, the failure mechanism is phonon instability. Borophene has enormous promise in the creation of composite materials and flexible devices as a 2D material with extraordinary flexibility, high ideal strength and outstanding elasticity. These findings suggest that by altering the concentration of hollow hexagons and mastering the borophene instability mechanism, the characteristics of borophene may be adjusted.

Electrical properties: Consider their band structures and the temperature dependence of the electronic conductivity for a more rigorous definition of these elements' (and many compounds') electronic characteristics. Metals contain partially filled energy bands, which means that the Fermi level crosses a partially filled band, as previously explained. Metals become worse conductors as temperature rises because lattice vibrations (referred to as phonons in physics) scatter the mobile valence electrons. At higher temperatures, semiconductors and insulators with full and empty bands, on the other hand, become better conductors because some electrons are thermally driven to the lowest unoccupied band. The difference between insulators and semiconductors is arbitrary, because all semiconductors are insulators in terms of metal-insulator transitions. If the band-gap (E_{gap}) of an insulator is less than around 3 eV, we call it a semiconductor. Single sheets of sp^2-bonded carbon (graphene) and elemental borophene are examples of semimetals with a band-gap around zero. Semimetals, like narrow gap semiconductors, have better conductivity at higher temperatures. The most stable shape for the electron-deficient B element is a combination of hexagonal and triangular structures [52] with two and three centre bonds, respectively [50]. Although not as stable as graphene, borophene possesses certain unusual electrical characteristics, including metallicity, Dirac-Fermi phenomena, superconductivity and semiconductivity.

Metallicity: In contrast to the semiconductor or insulating features of 3D bulk allotropes, of which only a tiny portion can transform into metal under ultrahigh pressure [76], Yakobson *et al.* [77] theoretically predicted that all polymorphs of borophene are metallic. Regarding that it was experimentally confirmed that the p_z orbit determines metallicity [39]. Wu *et al.* [57] used scanning tunneling spectroscopy to measure the electronic states of the successfully synthesized 12 and 3 phases and discovered that there are local densities of states around the Fermi level, demonstrating the energy band structure of metallicity. Using angle-resolved photoelectron spectroscopy, Matsuda *et al.* [64] observed the metallic boron-derived bands of 12 and inferred an interesting phenomenon-the coexistence of electronic pockets and hole pockets at the Fermi level, according on first-principles calculations, which also indicates its metallicity. Furthermore, Fazzio *et al.* [78] demonstrated that borophene's conductivity is anisotropic and that current transport in two perpendicular directions is directionally dependent.

Topological properties: Topological materials differ from ordinary materials in that they have numerous novel quantum features [79] and may be classified into three classes based on electron structures: topological insulators, topological semimetals and topological Dirac semimetals [80]. The electron structure of a topological Dirac semimetal is remarkable in that the energy bands at the Fermi level have 3D Dirac points and three neighbouring momentum orientations surrounding the Dirac points are all linear dispersion relationships. Because crystal symmetry protects band crossing properties, they have a lot of potential applications in electronic devices, semiconductors and other sectors [81]. Topological Dirac materials found so far typically contain heavy metal elements, which are plagued by a slew of issues that make them unsuitable for practical uses, such as pollution, excessive cost and material safety. As a result, light elements must be investigated in order to create stable topological materials. Dirac cones are found in graphene, a generally light Dirac material with a plethora of unexpected physical phenomena and electron properties identified by researchers.

Nowadays, topological properties research is no longer limited to the Weyl or Dirac fermions models and symmetry analysis has expanded to include crystals with magnetic order

and interactions. Ezawa [52] recently hypothesized the existence of triplet fermions in 12 borophene and developed three-band theories for triplet fermions. All of the previous insights into the topological features of 2D boron materials provide a strong platform for future electrical application research [82].

Superconductivity: The relatively low atomic mass of boron can produce strong electron-phonon coupling and the metallicity of borophene can cause itself to produce a higher carrier concentration [83,84], both of which are important factors in the formation of conventional superconductors, demonstrating that borophene has the potential to become a superconductor. By theoretical studies, Yakobson *et al.* [11] anticipated its critical temperature to be Tc ≈ 10-20 K, which is substantially higher than that of graphene. Nonetheless, electron doping and tensile strain can cause borophene's superconductivity to be suppressed [85], making it difficult to determine the critical temperature of borophene in tests. However, once these issues are resolved, these features will give borophene in superconducting devices more design flexibility and convenience.

Semiconductivity: Because of the non-zero band-gaps, scientists have demonstrated that some phases of borophene contain semiconductivity [86-88]. Zeng *et al.* [89] discovered that α- and β-sheets (slightly buckled sheet) are both small-gap semiconductors with indirect band-gaps of 1.40 and 1.10 eV, respectively and that the α-sheet has the highest cohesive energy and is probably the most stable buckled borophene based on PBEO hybrid calculation results. Researchers discovered that by changing the applied stress, the surface band-gap of thicker borophene may be modified, producing a shift in electron mobility and converting the conductivity type of borophene from metallic to semiconducting. In this scenario, increasing electron mobility is as simple as altering the applied tension. Therefore, γ-B28 borophene has application prospects in the field of pressure-sensitive and photosensitive devices.

1D Nearly free electron states: Almost free electron (NFE) states have an effective mass that is nearly equal to the free electron mass, exhibit typical parabolic energy dispersion and have notable electron transport features that can be used in electron emitters [90]. The NFE states can be found on low-dimensional material surfaces with perpendicular confinement potentials, such as 0D C_{60} molecules, 1D nanotubes and nanoribbons [91] and 2D graphene, but due to the presence of a potential gradient that is usually normal to the material's basal plane, these NFE states prefer to extend in the vacuum region rather than stay around the basal plane, limiting their superiority in transport properties.

Using STM and first-principles computations, Wu *et al.* [57] found delocalized 1D NFE states in an Ag(III) supported borophene homojunction, which consists of two (2,3) domains (*i.e.*, the v1/6 or 12 sheet) interconnecting the two (2,2) ribbons as a line defect. The NFE states in borophene are distinc from those in the other low-dimensional materials discussed above; the former are still kept near the borophene surface due to the as-formed in-plane potential gradient and experience less disturbance along the plane's perpendicularity. Because of this one-of-a-kind process, the NFE states in borophene can be used in charge transport.

Thermal properties: Borophene has remarkable thermal qualities, including as thermal conductivity and thermal stability. Studies in recent years have revealed that its thermal properties are closely related to the structure of borophene.

Many forms of borophene have been theoretically predicted and experimentally proven in recent years, including the β_{12}, δ_6 and χ_3 phases, which were produced epitaxially on Ag(111). They may be thermally unstable if removed from the substrate, especially the δ_6 phase. Zhou & Jiang [92] devised two efficient empirical potentials for molecular dynamics simulations to figure out the interaction between low-energy triangular structures and borophene in order to manage the instability of δ_6 phase borophene: the linear potential valence force field mode and nonlinear Stillinger-Weber potential.

Because borophene is made up of the same boron atom, the phonon frequencies of various borophene phases are similar. Despite this, the amount of boron atoms in each unit cell varies, resulting in varied geometric symmetries and varying numbers of optical phonon branches, leading to diverse thermal transport [93]. The phonon transmission in borophene is essentially isotropic for low-frequency phonons, similar to graphene, but one-dimensional for high-frequency phonons, resulting in ultrahigh thermal conductivity. This suggests that the observed variations in thermal conductivity and thermal characteristics are due to differing phonon scattering speeds. For example, β_{12} phase is isotropic, whereas α phase is very anisotropic; α phase is fundamentally stable, whereas δ_6 phase is thermally unstable [94].

The unique thermal properties of borophene provide insight into the potential applications of these materials, which can suit the needs of a variety of sectors. High thermal conductivity, for example, can aid in the removal of stored heat in solar and electronic equipment, whereas low thermal conductivity materials are required in the thermoelectric and thermal insulation industries. Because borophene has a wide range of heat transport properties, it can be used in thermal management and transparent conductors.

Synthetic methods

Synthesis of graphene: Since graphene was isolated in 2004 by Geim & Novoselov [4] using famous Scotch tape method, there have been many processes developed to produce few-to-single layer graphene. One of the primary concerns in graphene synthesis is producing samples with high carrier mobility and low density of defects. To date, there is no method that can match mechanical exfoliation for producing high-quality, high mobility graphene flakes. However, mechanical exfoliation is a time consuming process limited to small scale production. There is a great interest in producing large-scale graphene suitable for applications in flexible transparent electronics, transistors and so forth [95]. Some concerns in producing large scale graphene are the quality and consistency between samples as well as the cost and difficulty involved in the method.

The two major ways for preparing 2D nanomaterials are "bottom-up" and "top-down" procedures. Physical vapour deposition (PVD), chemical vapour deposition (CVD) and wet chemical synthesis processes [96], among others [97], are

examples of the "bottom-up" approach. CVD is the process of forming a film on a substrate by reacting related gas phase precursors. Three critical aspects determining the qualities and development of the products in this process are the environment, substrates and precursors. CVD was used to make graphene, a metal oxide. The material source is vapourized into a gaseous state using a physical approach under vacuum circumstances and deposited onto a substrate to form a functional film during the PVD process. Chemical processes in solution are commonly used to make 2D nanosheets of non-layered materials, a process known as wet chemical synthesis.

Almost all forms of 2D nanomaterials can be synthesized using bottom-up techniques in general. Mechanical cleavage [72,98], ultrasonication [73], ion intercalation exfoliation [98] and etching [57,79,98] are examples of "top-down" methods. Mechanical cleavage is a technique for exfoliating 2D structures from bulk materials that uses shear pressures to overcome van der Waals interactions between connection layers [1,2,7,72]. This process was used to make graphene for the first time [30]. Based on shear forces, ultrasonication promotes liquid exfoliation. Its acoustic energy can delaminate layered materials like graphite and MoS_2. The size, quality and dispersion of 2D materials can be adjusted with this method by varying the sonication solvent and time. Ultrasonication has the advantages of low cost and wide manufacturing scale, however single layer 2D material yield is limited.

Mechanical exfoliation: Developed by Geim & Novoselov [4], highly oriented pyrolytic graphite (HOPG) is used as a precursor in the exfoliation process. Oxygen plasma etching was used to form 5 m deep mesas in the HOPG, which were then pressed into a layer of photoresist. The HOPG was cleaved off the photoresist after it was baked. Scotch tape was used to pull graphite flakes from the mesas repeatedly [4]. These thin flakes were then trapped on the surface of a Si/SiO_2 wafer after being discharged in acetone [99]. The contrast difference in an optical microscope and single layers in a SEM were used to identify these few-layer graphene (FLG) flakes. Geim & Novoselov [4] abled to create single- and few-layer graphene flakes with dimensions of up to 10 μm using this method.

Chemical vapour deposition: The most popular and current way of manufacturing graphene molecularly is chemical vapour deposition (CVD), which is growing increasingly popular since it can manufacture graphene with a large surface area. Graphene is deposited onto a transition metal substrate that is easily etched by an acid solution and can thus be transferred to another substrate, such as silicon dioxide, using this method. This opens up the possibility of using graphene for a variety of applications that could eventually replace silicon technology. Low sheet resistance per square of graphene over a copper substrate, on the other hand, combined with high optical transparency, could result in excellent transparent conductive films. In contrast to thermal graphene breakdown, where carbon is already present in the substrate, chemical vapour deposition (CVD) uses carbon as a gas and a metal as both a catalyst and a substrate to build the graphene layer.

Growth on nickel: Harack *et al.* [23] grew few-layer graphene sheets on polycrystalline Ni foils. The foils were initially annealed in hydrogen before being exposed for 20 min at 1000 ºC in a CH_4-Ar-H_2 atmosphere at atmospheric pressure. The foils were then chilled at varied rates ranging from 20 to 0.1 ºC/s. The thickness of the graphene layers was discovered to be dependent on the cooling rate, with 1 ºC/s producing few layer graphene (usually 3-4 layers). Cooling at a faster rate results in thicker graphite layers, but cooling at a slower rate prevents carbon from separating to the Ni foil's surface. The graphene layers were transferred to an insulating substrate by first coating the Ni foil with graphene in silicone rubber and covering it with a glass slide and then etching the Ni in HNO_3.

Growth on copper: A similar method was utilized by Li *et al.* [30] to create large-scale monolayer graphene on copper foils. Copper foils with a thickness of 25 m were heated to 1000 ºC in a flow of 2 sccm hydrogen at low pressure before being exposed to a methane flow of 35 sccm and a pressure of 500 mtorr. The graphene is largely monolayer, according to Raman spectroscopy and SEM imaging, regardless of growing duration. This shows that the process is self-limiting and surface mediated. They used graphene to create dual gated FETs with a carrier mobility of 4050 $cm^2 V^{-1} s^{-1}$. A roll-to-roll procedure for producing graphene layers with a diagonal of up to 30 inches and transferring them to transparent flexible substrates was recently demonstrated [100]. CVD was used to develop graphene on copper and the graphene-copper was then covered with a polymer support layer. Chemical etching was used to remove the copper and the graphene layer was subsequently transferred to a polyethylene terephthalate (PET) substrate.

Molecular beam deposition: Using a molecular beam deposition approach, Yu *et al.* [101] abled to grow graphene layer by layer. Fig. 7 shows a diagram of the setup as well as a TEM image of the graphene produced. The gas was broken down at 1200 ºC using a thermal cracker and placed on a nickel substrate, starting with an ethylene gas source. At 800 ºC, large-area, high-quality graphene layers were created. This process allows for the production of one to multiple layers of graphene by creating one layer on top of another. The amount of graphene layers formed was found to be independent of cooling rate, indicating that carbon was not absorbed into the bulk of the nickel as it is in CVD nickel growth. Raman spectroscopy and TEM [102,103] were used to confirm the findings.

Unzipping carbon nanotubes: By suspending multi-walled carbon nanotubes in sulphuric acid and then treating them with $KMnO_4$, they were sliced lengthwise. This resulted in oxidized graphene nanoribbons, which were then chemically reduced. Due to the existence of oxygen defect sites, the resulting graphene nanoribbons were found to be conductive but electrically inferior to large-scale graphene sheets [104].

Sodium-ethanol pyrolysis: Graphene was made by heating sodium and ethanol in a sealed jar at a 1:1 molar ratio. The result of this process is pyrolyzed, yielding a substance made up of fused graphene sheets that can be freed *via* sonication. This resulted in graphene sheets of up to 10 μm in length [105]. TEM, selected area electron diffraction (SAED) and Raman spectroscopy were used to confirm the individual layer, crystalline and graphitic nature of the samples.

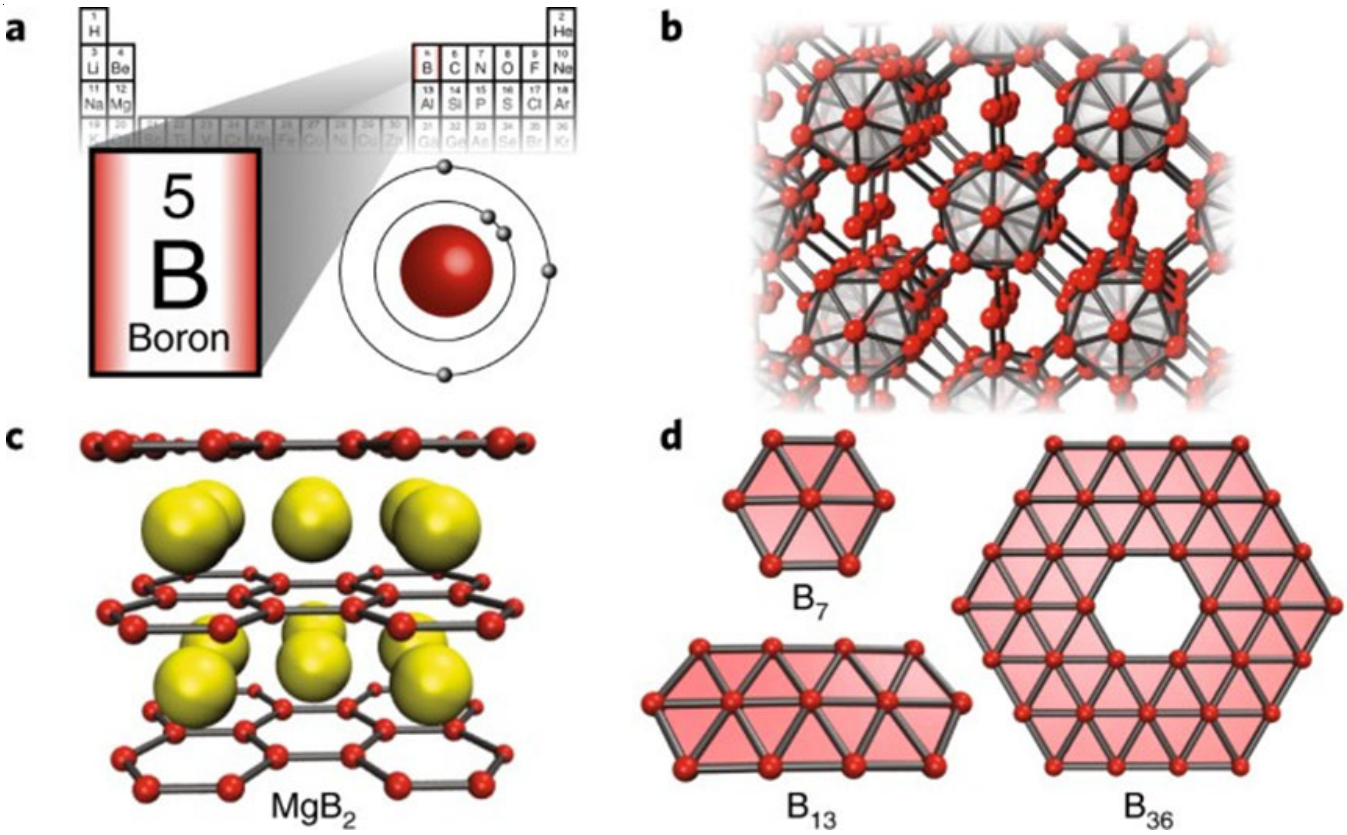

Fig. 7. 2 D material boron

Graphene oxide: The sonication and reduction of graphene oxide is another method for producing graphene (GO). Graphite oxide is hydrophilic due to the polar O and OH groups generated during the oxidation process and it can be chemically exfoliated in a variety of solvents, including water [106-108]. After that, the graphite oxide solution can be sonicated to generate GO nanoplatelets. The oxygen groups can then be removed using one of several reducing agents in a reduction process. Stankovich *et al.* [109] used a hydrazine reducing agent in this procedure, however the reduction was found to be incomplete, leaving some oxygen behind. The precursor to graphene production is graphene oxide (GO). GO is beneficial because, unlike graphite, its individual layers are hydrophilic. To create single- or double-layer graphene oxide, GO is suspended in water by sonication [110], then coated onto surfaces by spin coating or filtration. The graphene oxide is subsequently reduced, either thermally or chemically, to produce graphene films. Although there is great consensus on the overall types and proportions of oxygen bonds present in the graphene lattice, the specific structure of graphene oxide is still a matter of discussion [111].

Other techniques: Electron beam irradiation of PMMA nanofibres [112], arc discharge of graphite [113,114], thermal fusion of PAHs and conversion of nano diamond are some of the various approaches to make graphene.

Synthesis of borophene: Multiple oxidation and exfoliation can be used to remove substances on the surface of a material, resulting in nanosheets. This approach was successful in producing borophene [36]. The most common method for making 2D nanosheets is CVD, PVD and wet chemical are examples of bottom-up methods [115]. Mechanical cleavage, ultrasonication, ion intercalation exfoliation, selectively etching and thermal oxidation etching are examples of top-down methods.

Synthesis on Ag(III): Guisinger *et al.* [11] used boron vapour (99.9999% purity, boron flux controlled at 0.01 to 0.1 monolayer per min [ML min^{-1}]) as the boron source to successfully synthesize ultrathin monoatomic layer borophene on clean silver at temperatures between 723 and 973 K, under ultrahigh vacuum conditions.

The usage of harmful precursors (*e.g.* diborane) was avoided due to the high-purity boron atom source and the clean silver substrate offered an excellent inert surface for the formation of borophene [36]. At 820 K, this approach resulted in the creation of two phases of borophene: a homogenous phase and a more corrugated "striped" phase. The relative concentrations of the two phases were demonstrated to be affected by both temperature and deposition rate, with low deposition rates favouring the creation of striped phase and greater deposition rates favouring the generation of homogenous islands [116]. Furthermore, the creation of the striped phase was temperature dependent, with the existence of this phase being limited at 720 K and almost entirely striped at 970 K (atomic-scale structure and growth mode of striped phase).

Synthesis on Al(III): With a long-awaited planar hexagonal honeycomb structure, Wu *et al.* [57] made a big breakthrough in the synthesis of borophene. Under ultrahigh vacuum conditions, monoatomic layer borophene was formed on an Al(III) substrate using boron vapour with a purity of 99.9999%

at a deposition rate of 0.1 ML min^{-1} (temperature: 500 K). As a result, a successful borophene synthesis with a honeycomb structure would be very interesting [115].

Synthesis on Au(III): Guisinger *et al.* [11] succeeded in synthesizing borophene on Au(III) substrate and investigated the effect of varied temperature Au(III) substrates on the thermal deposition of boron atoms [116]. Unlike the production of borophene on Ag(III), Cu(III) [117-119] and Al(III) substrates, boron atoms dissolved into gold atoms at high temperatures (equivalent to or more than 823 K) and then segregated to the surface to produce borophene after cooling on the Au(III) substrate. Nanoscale borophene islands were discovered on the surface of Au(III) during the borophene synthesis process. As a boron concentration increased, the trigonal network was broken down, resulting in bigger borophene islands on the substrate surface. According to current research, the bigger the boron atom concentration, the larger the size of borophene. However, due to the difficulties of transferring borophene from metal substrates, its future applications are limited. Because of the weak bonds and minimal charge transfer created on the surface between Au(III) and borophene, borophene was easily peeled off, allowing for continued application.

Effect of metal substrate on borophene synthesis: The nucleation energy barrier limits material formation in classical nucleation theory, however the 2D boron nucleation barrier is higher than its 3D bulk structure, inhibiting natural nucleation of borophene [120-124]. The difficulty of synthesizing borophene is exacerbated by its thermodynamic defects and polymorphism. As a result, lowering the 2D boron nucleation barrier and inducing 2D nucleation offers an energy-efficient method to borophene synthesis [125]. The interaction between metal substrates and boron, according to Yakobson *et al.* [11], aids the nucleation of boronene because the 3D nucleation barrier of boron on some metal substrates is larger than the 2D nucleation barrier. Then there's the question of what kind of substrate to use for borophene production. For the selection of appropriate metal substrates, two criteria have been proposed (i) the substrate should have a little solubility in boron atoms and (ii) the binding force between the substrate and the boron atoms should be moderate [98]. It is difficult to pull borophene away from the substrate if the force is too powerful and borophene can readily create a boride if the force is too strong. Boride can be easily produced when borophene is synthesized on Fe, Co or Ni substrates [126].

The generally utilized substrates may be split into two primary categories based on their interaction with borophene: one has a high binding energy and large charge transfer with borophene, such as Mg (0001), Al(111) and Ti (0001) [127]. Except for a Fermi level shift, the profile of (inplane) bands of hexagonal borophene produced on these substrates is similar to that of its free standing phase. The other has a lower binding energy with borophene such as Au(111) and Ag(111) and hexagonal borophene's in-plane bands divide into multiple sub-bands [57]. Xu *et al.* [32] theoretically examined the nucleation mechanism and growth process of borophene on the surface of Ag(111) and experiments proved that the best stable structure is one in which the hollow hexagons are aligned in parallel and the hollow hexagon concentration is 1/6. On the Cu(111) surface, Zhao *et al.* [128] discovered that 2D dense boron clusters were easily produced. Additionally the lower the formation energy will be the larger the cluster size. As a result, the metal substrates have a significant impact on the structure of the generated borophene and it is critical to choose the right substrate for the purpose.

Effect of temperature and deposition rate on borophene synthesis: In theory, boron's 3D structure is more stable than borophene's, making it easier to produce. As a result, one of the most important steps in the production of borophene is inducing boron atoms to choose 2D nucleation. The external growth environment has a significant impact on the nucleation barrier of materials, impacting the free energy of boron growth-boron atoms can only grow to a given structure if the free energy is greater than the nucleation barrier. Because the free energy of boron growth is substantially lower than the nucleation barrier of borophene, the necessary 2D structure cannot be achieved at low temperatures. Similarly, the free energy of boron growth is substantially higher than the 3D boron nucleation barrier, boron atoms tend to develop into a 3D structure when the temperature is too high. As a result, in order to synthesis borophene, the temperature must be carefully managed so that the free energy of boron growth remains between the 2D and 3D nucleation barrier's energy regions. Wu *et al.* [57] demonstrated that distinct phases of borophene can be produced at various temperatures. Controlling crystallization quality and borophene coverage also requires real-time monitoring and detection of the atomic deposition rate. Guisinger *et al.* [11] discovered that a slower deposition rate helped to establish a fringe phase (β_{12}). The synthesis of borophene in Ag by Gozar *et al.* [129] revealed that the deposition rate had a significant impact on the crystallization of 2D materials (111). When continuous deposition exceeds, the crystallinity of the material would decrease. As a result, the deposition rate and amount of raw materials must be tightly controlled in accordance with actual needs.

Effect of solvents on borophene synthesis: Temperature has no effect on the production of borophene in the top-down synthesis technique, however variations in the selected solvent can directly impact the size and thickness of borophene [130]. The exfoliation mechanism of borophene is determined by the polarity of the solvent, which affects the size, thickness and layers. Sonochemical exfoliation was used to successfully synthesise borophene and the influence of various solvents (acetone, ethylene glycol, water, isopropyl alcohol and DMF) on the synthesis of borophene was investigated [131]. According to Vinu's *et al*. work [132], ethylene glycol and acetone exhibit intercalation-mediated exfoliation and are conducive to the formation of borophene monolayers, with acetone outperforming ethylene glycol. Other solvents, on the other hand, rarely yield monolayers due to their different exfoliation mechanisms, DMF (yields multilayered borophene) and water (which yields few monolayers) tend to mediate borophene surface exfoliation, whereas isopropyl alcohol (which yields few monolayers) fragments exfoliation.

Applications: There are currently numbers of applications that shows advantage of borophene's unique features, such as:

Flexible electronics: Scaled-down hybrid electronic devices that take advantage of the superior properties of 2D materials may be possible. If borophene was put to an elastomeric substrate, researchers believe its distinctive undulating structure would confer considerable stretchability. To put it another way, it may be conceivable to make borophene-based devices that can be deformed and then returned to their original shape. Because borophene is conductive, it could be an excellent material for flexible electronic devices. One of the major issues facing researchers is that like many 2D materials [126], borophene is extremely sensitive to the external environment and it has yet to demonstrate long-term stability and reliability in electrical systems [132]. In order to comprehend the probable failure modes in electronic devices, researchers are now developing new imaging techniques to capture the mobility of individual atoms in 2D materials [133].

A substantial body of theoretical and experimental evidence suggests that borophene has good properties and has the potential to be used in a variety of sectors, including energy storage [134], electronic devices [135,136] and biomedicines [137]. The size and physico-chemical properties of borophene are important factors in its future use in electrical devices and other disciplines. However, large-scale laboratory manufacturing of borophene with a huge surface area remains a challenge. The currently synthesized borophene is small in size (nanometer level) and unstable in the free state, posing challenges to its continued use in electronic devices, but it has shown promise in biomedicines. In the realm of tumour therapy, nanoscale materials are very popular. Since tumours have an elevated permeability and retention (EPR) effect, drug carriers with diameters ranging from 10 to 1000 nm will be concentrated at the tumour site to achieve passive tumour targeting, improve medication efficacy and reduce adverse effects [138]. Furthermore, free borophene is easy to stabilize by combining it with other elements or groups, giving it a significant advantage in drug administration. To ensure correct release at the tumour site or improve the stability of the delivery system in the body, intelligent drug delivery frequently necessitates the modification of unique groups on the carrier. The addition of specific groups to borophene cannot only give a boron drug carrier new functions, but it can also solve boron's stability problems.

Supercapacitors: The supercapacitor is a novel form of energy storage device that has the following unique characteristics: low cost, extended cycling life, fast charge/discharge rate, high power density and low energy density. The electrical conductivity and surface area of the electrode materials have a significant impact on supercapacitor performance due to the surface charge-storage process. Recent advancements in 2D nanomaterials have resulted in a variety of supercapacitor candidates with ultrahigh electrical mobility, enormous surface area and ultrathin thickness [24].

Batteries: Because of its metallic characteristics and low atomic weight, borophene can be used as a battery anode. The stability of the overall system remains high or even improves when the intrinsic hollow hexagonal vacancies in borophene securely hold adsorbed metals like lithium and sodium, according to theoretical research [139]. More importantly, borophene exhibits none of the drawbacks associated with typical anode materials such as $NiCo_2O_4$, hard carbon and Sn [140], such as significant volume expansion, slow kinetics and low intercalation usefulness. In summary, as expected theoretically, borophene has the following advantages as an anode, particularly for Li- and Na-ion batteries [119,141].

Stable conductive properties: The *Pmmn* borophene has a unique buckling structure, in which the boron atoms can be classified into two groups based on their location heights: peak and valley [36]. The layer structure is loosely packed, allowing for a slight volume expansion (less than 2%) and lattice modification when varied quantities of metal atoms such as sodium and lithium are embedded in it. As a result, borophene can be used as a battery anode material with good structural integrity and cycle stability.

Extraordinary rate capability: Xu *et al.* [142] calculated an ultralow diffusive energy barrier (0.0019 eV) of sodium in the valley direction based on the peculiar structure of borophene, which is substantially lower than that of typical anode materials such as $Na_2Ti_3O_7$ and Na_3Sb (0.19 and 0.21 eV, respectively). Surprisingly, the diffusion rate in that direction was almost 1000 times that of $Na_2Ti_3O_7$ and Na_3Sb. Finally, due to its anisotropic diffusion features, Li's diffusion energy barrier was somewhat higher than that of Na. All of these findings suggest that borophene, as the anode of Li- or Na-ion batteries, has a remarkable rate ability, which can clearly answer the problem of slow kinetics.

Ultrahigh theoretical capacity: When Na/B (borophene) ratio hits 0.5 (sodium totally uniformly covers the upper and lower sides of borophene), the theoretical capacity reaches a maximum (1218 mAh g^{-1} Na0.5B), which is roughly three times larger than the graphite anode (372 mAh g^{-1}). The situation is considerably better for lithium (Li0.75B), which has a greater atomic radius and a theoretical capacity of 1860 mAh g^{-1}, which is nearly four times that of graphite anode [113]. As a result, borophene can greatly improve metal intercalation utility, resulting in higher battery energy and power densities.

Effectively avoiding the dendrite formation: Dendrite concerns affect both Li and Na-ion batteries, which include highly reactive metals with low melting temperatures, posing a severe safety concern that has yet to be properly addressed. Borophene, on the other hand, may be able to reverse this. The calculated average open-circuit voltage of a Na-ion battery using borophene as anode material is as low as 0.53 V during charging, according to the researchers and the link between borophene and sodium is strong [83]. Metal atoms uniformly coated borophene rather than clustering to form a separate metal phase in both cases, thereby inhibiting dendrite growth while retaining a high energy density [140].

Hydrogen storage: The development of a material appropriate for hydrogen storage is critical in light of finite fuel supplies and environmental concerns. Two indices are needed to evaluate a material's hydrogen storage ability: adsorption energy and hydrogen adsorption capacity. In terms of adsorption energy, a value in the range of 0.2-0.6 eV is required to ensure that hydrogen molecules can be adsorbed on the surface of materials in a stable and easy manner. With its advantages

of light weight and huge specific surface area, borophene has been identified as a contender for H_2 storage, particularly when combined with graphene or transition metals [45,59]. Fortunately, chemical activity may be increased and the contact between borophene and H_2 can be intensified with the use of alkali or transition metals.

Bioimaging: Bioimaging, which includes fluorescence imaging [143,144], photothermal imaging [145] and photoacoustic (PA) imaging [146-149], can offer information on the location and size of tumours. Each imaging mode displays different lesion information and each imaging mode has its own set of benefits and drawbacks. As a result, a tumour multimodal imaging platform can provide more comprehensive tumour information, which can considerably reduce the chance of misdiagnosis.

Scientists recently developed a borophene-based tumour multimodal imaging platform that can do fluorescence imaging, PA imaging and photothermal imaging all at the same time [116]. The fluorescent material is placed onto the carrier and active or passive targeting methods are used to enhance the formulation at the tumour. When compared to optical and acoustic imaging, PA imaging improves probing depth, picture contrast and spatial resolution while overcoming many of the drawbacks of these two imaging modalities [116].

Drug delivery: The key to reducing chemotherapy side effects is to release chemotherapeutic medicines locally. As a result, developing a smart tumour microenvironment responsive drug-release platform is critical. The ultrahigh specific surface area of borophene allows for drug loading and anchor points for functional group modification, making it a good material for anticancer treatment in many ways [116].

Cancer therapy: Photothermal therapy can be used to treat cancer in a non-invasive or minimally invasive manner. The approach irradiates tumour tissue with near infrared (NIR) radiation, which causes tumour tissue temperature to rise due to photothermal conversion, resulting in tumour cell death [150, 151]. Low toxicity, significant light absorption, high photothermal conversion efficiency and photothermal stability in the NIR window (650-950 nm) are all desirable characteristics of a photothermal therapeutic drug. Researchers utilized borophene in tumour photothermal therapy and found that it was effective [115]. Photothermal conversion efficiency, photothermal stability and UV absorbance are three critical criteria for an excellent photothermal agent and these properties of borophene were examined borophene has a strong UV-vis-NIR absorption. The temperature variations of borophene at different concentrations were measured after it was disseminated in an aqueous solution and treated with 808 nm infrared light (2 W cm^{-2}) for 5 min.

Biosensors: Biosensors can detect biomarkers such as hormones, proteins and glucose rapidly and precisely with high specificity and sensitivity [152] and used for blood sample detection, early cancer diagnosis and clinical analysis, garnering a lot of interest in the biomedical area. Due to their improved electrochemical performance, high surface-to-volume ratios, more surface-active sites and high electronic mobilities at monolayer thicknesses, 2D nanomaterials have become good options for biosensors.

Because of its wide surface area and excellent absorbability to gas molecules, borophene has a lot of biosensing application potential for gas detection. It can monitor not only non-hazardous gases like ethanol and ammonia [153], but also toxic gases like formaldehyde, CO and NO, which graphene and phosphorene gas biosensors, both of which have lately been deemed highly sensitive as biosensors, cannot [154]. Apart from the relatively significant adsorption strength of highly poisonous gases on borophene surfaces, the electronic bandgap, which other 2D materials such as graphene lack, is one of the reasons why borophene is better suitable for highly toxic gas biosensors. When the gas adsorbs, the electronic bandgap of borophene rapidly decreases, allowing a large number of electrons to transfer and increasing electrical conductivity. This makes borophene particularly useful in the development of highly dangerous gas biosensors [155].

As a result, further comprehensive research will be required to clarify the cytotoxic effects, durational stability and impacts while in close contact with biological tissues, among other things, in order to accomplish the transformation of borophene biosensors in the biomedicine sector [156]. Furthermore, because borophene is unstable when exposed to air, it is vital to address potential external interactions, such as reactivity with metallic objects or smoking byproducts.

Battery electrodes: Because of its high storage capacity and electrochemical performance, boron is a suitable electrode material for lithium-ion and sodium-ion batteries. According to a recent study, borophene has the largest storage capacity of all the 2D materials studied so far [119].

Catalysis: Due to their unique features, such as enormous surface areas and novel electronic states, 2D materials hold considerable promise for application as catalysts. Borophene is a catalyst that can be utilized in hydrogen evolution, oxygen reduction and carbon dioxide electrochemical reduction [157]. The electrochemical reduction of carbon dioxide, in particular, offers significant potential in terms of aiding climate change initiatives. However, due to a dearth of reliable and efficient catalysts, development has been slow.

Hydrogen storage: Demand for energy storage and the evolution of hydrogen and fuel cell technologies have prompted further study into hydrogen storage systems in recent years [125]. Borophene has been demonstrated to have a high hydrogen storage capacity, thanks in part to the boron atoms' low mass. The molecular hydrogen binding energy to the boron sheet is higher than that of graphene [125].

Gas sensors: Because of its gas adsorption capabilities, borophene is useful in gas sensing applications [157-161] for ethanol, carbon monoxide, phosgene and formaldehyde. Due to their distinctive electrical structures and enormous surface-area-to-volume ratios, 2D materials have shown tremendous potential for the creation of gas sensors.

Perspectives: Despite the challenges, borophene has a lot of potential applications in advanced composite materials, flexible electrical goods, energy storage materials and biomedicine, thus it's worth looking into [41]. Most previous research had concentrated on the development and implementation of borophene in electronic devices, with only a few

studies addressing the materials' potential in biomedicine [13]. Boron is required for the creation of ribonucleic acid, an important building block of life, suggesting that it may have played a role in the start of life. Ancient Chinese medicine employed naturally produced borax ($Na_2B_4O_7{\cdot}10H_2O$) to treat acute tonsillitis, pharyngitis, stomatitis and gingivitis [13]. Borophene is now widely used in cancer diagnosis and treatment due to its extraordinarily high specific surface area, outstanding biocompatibility, high photothermal conversion efficiency and good bioimaging properties [130]. Boron and its associated compounds have made a significant contribution to human health since ancient times and there is reason to expect that boron-related products could make a significant difference in biomedical sectors [137].

Potential applications of borophene in the field of biomedicine: In addition to the photothermal therapy, drug administration, tumour multimodal imaging and other activities, borophene is predicted to be used in a variety of fascinating biomedical applications. In recent years, tumour vaccinations have received a lot of attention. They have fewer adverse effects than chemotherapy and radiotherapy and they can inhibit tumour growth, dissemination and recurrence by boosting the patient's own immune system [137]. However, current tumour vaccines have issues such as difficulty collecting immune-related cells, ineffective antigen delivery and ineffective tumour killing capabilities [116]. Using oxidized graphene (2D material) as a chassis, many researchers have developed a "one-size-fits-all" tumour vaccine delivery platform that incorporates antigen presenting cell (APC) recruitment/activation, antigen transport and cross-presentation to tackle the existing challenges with tumour vaccines [116]. The 2D oxidized graphene promotes APCs and subsequent antigen cross-presentation more effectively than 0D spherical nanocarriers and serves as an immune-related cytokine and antigen reservoir [116]. When oxidized graphene reaches macrophages, it folds and neatly wraps the antigen in wrinkles to shield it from the enzymes in the envelope, according to experiments [116]. Furthermore, autophagy, APC activation and effective antigen cross-presentation are all linked to the folding properties of oxidized graphene. Furthermore, as a 2D nanomaterial, oxidized graphene has a unique dimension that can provide a nano-biointerface effect that is unlike that of regular spherical rod-like nanomaterials [162]. As a result, 2D materials hold a lot of promise in terms of helping immunotherapy. Borophene, as a 2D material with great mechanical toughness and flexibility, is extremely likely to have outstanding immunological function, including cytokine-like activity, enzyme like activity and agonist action similar to oxidized graphene, making it a possible immunotherapy drug delivery platform [162].

Brain tumours are difficult to treat lesions, however boron neutron capture therapy (BNCT) has demonstrated to be effective in treating them [163]. It works by enriching the stable isotope boron-10 (10B) in tumour cells, then irradiating them using neutron beams to trigger nuclear capture and fission events, which kill cancer cells [164]. It has the following advantages over standard radiotherapy and chemotherapy: (i) tumors have a much higher affinity for boron-containing drugs than normal tissues, leading to tumor-targeted therapy; (ii) BNCT has a good killing effect on both oxygen-rich and hypoxic tumours, avoiding the need for oxygen-dependent radiotherapy; (iii) it has a good killing effect on both oxygen-rich and hypoxic tumours, avoiding the need for oxygen-dependent radiotherapy; (iv) has a good killing effect on both oxygen; (v) BNCT's killing impact is independent of the cell growth cycle and effective for tumour cells in the stationary phase, unlike chemotherapy and radiotherapy, which are dependent on the cell growth cycle. As a result, BNCT is regarded as a more advanced anti-tumor radiation technique. Nonetheless, achieving a high concentration of boron carriers in tumours is an essential prerequisite for BNCT technology, which necessitates careful design and selection of boron carriers [165]. Borophene, which has good tumour targeting and photothermal effects and has better boron purity than other boron containing compounds, is anticipated to become a possible borophene application.

Superior properties of borophene: As predicted theoretically, despite the fact that its parent atom, boron, is an unambiguous non-metallic semiconductor, these are metallic sheets at the nanoscale. Furthermore, like graphene, the new film is robust and flexible, with good electronic conductivity, but it is mechanically much stronger and weights significantly less due to its low mass density, making it a treasure indeed [166]. The flexibility is significantly greater than graphene's and has been described as "record high." Its optimum strength outperforms all previously known polymer materials. It also has a higher stiffness-to-weight ratio [120]. In fact, when borophene is subjected to strain, it refuses to fracture and instead undergoes strain-specific phase transitions in its structure, making it even stronger.

Researchers in flexible electronics, such as flexible electrodes and nanoelectronic connections, have noticed a peculiar wavy or corrugated surface when it grows on a silver substrate, which has piqued their interest [13]. Its strength and lightness make it a good candidate for use as a reinforced component in composites. In the domain of 2D nanoelectronic materials, it is so unique. It possesses two distinguishing properties that may account for its unusual qualities [13]. The boron atom network, for example, is made up of highly variable hollow hexagons that create a reference triangle lattice. Customizing the hollow hexagon content allows to customize this lattice for desired mechanical properties [40]. In other words, the lattice becomes stronger as more hollow hexagons are introduced. Another trait is the delocalized multi-center bonding, which gives it a very metallic appearance, a development that has yet to be thoroughly explored. It's also important because of its superconducting. According to certain studies, it has a higher electron density than graphene, implying that it might conduct electricity with negligible losses if cooled [48].

Due to the high reactivity of boron, a free-standing sheet of borophene has remained elusive thus far. This would necessitate a more precise measurement of its conductivity, which has not been accomplished thus far. However, the reactivity of boropheneis far from a disadvantage, since it may make simple to optimize its properties by modifying it with other

chemical groups or sandwiching it between sheets of other material [13]. Because of boron's hardness, borophene has the potential to be a more durable material for different purposes than silicene and germanene, which are easily torn. With such extraordinary properties, not surprisingly that this wonder material has a wide range of applications, from electronics to other photovoltaic devices [12]. Scientists have developed stable boron and hydrogen atom nanosheets that could be used in nanoelectronics and quantum information technology [14].

Despite the fact that borophene is usually likened to its super-material forerunner graphene, borophene is far more difficult to produce. Graphene is a layered substance made up of stacks of two-dimensional sheets that is atomically thin. Scientists peel off a two-dimensional layer of graphite to remove it [167]. Boron, on the other hand, is not layered when it is purchased in quantity. Hersam *et al*. [167] made borophene for the first time a few years ago by growing it directly on a substrate. However, the produced material was very reactive, rendering it prone to oxidation. This is the first manmade product (not a natural product) that combines extreme hardness with amorphous structure. Boron, on the other hand, lacks the strength of a good-quality diamond. It easily rubs off on the diamond lap as well as the carborundum wheel. Boron is a very volatile element, with a vapour tension of around 1800 ºC. It can, however, be easily fused both at atmospheric pressure and in vacuum.

The second approach relies on the hydrogen breakdown of boron chloride at high red heat [168]. This process can take place in one of two ways: (i) in an arc discharge between two boron or water-cooled copper electrodes in an environment of boron chloride and hydrogen; or (ii) by deposition on a hot graphite tube heated by current running through it. One method of measuring radiant energy would be to calculate the radiant energy input as the difference between electrical energy inputs before and after the radiant energy strikes the boron component. The fact that the boron piece's resistance is the same indicates that its temperature is the same. Researchers have been looking for 2D materials having honeycomb structures like graphene, or monoelemental 2D nanosheets in the same group as or close to carbon, in the hopes of developing graphene like materials with great qualities in recent years [104].

Borophene as a new wondor material: As a novel super material, borophene has received a lot of interest in recent years. In the last five years, the citation rate of borophene-related studies has risen dramatically. Comprehensive review articles on borophene, on the other hand, are uncommon [169] elaborates on the dominant structure of borophene formation under various conditions [170]; provides a good summary of how theory has guided the experimental synthesis of borophene and systematically analyses the future application prospects of borophene [171]. The preceding evaluations give a solid overview of the relationship between borophene's structure and properties, but the detail about the material's synthetic techniques or uses were discussed.

Graphene *versus* traditional materials: The properties of graphene is compared with more typical materials like 2D semiconductors in order to describe some of its fascinating characteristics:

(1) Graphene has a nominal band-gap of zero, whereas the other semiconductors have a finite band-gap. Normally, studying electron and whole transportation through a semiconductor necessitates using materials which were doped differently [135]. However, in graphene, the nature of a charge carrier changes from an electron to a hole or *vice-versa* at the dirac point. In graphene, the Fermi-level is always within the conduction or valence band, but in typical semiconductors, when pinned by impurity states, the Fermi level frequently dips within the band-gap [49].

(2) Graphene dispersion is chiral. This has something to do with some extremely different material phenomena, such as Klein tunnelling [172].

(3) Graphene has a linear dispersion relation, whereas semiconductors have a quadratic dispersion relationship. Many of graphene's remarkable physical and electrical properties can be explained as a result of this fact [3].

(4) Graphene is far thinner than a conventional 2D electron gas (2DEG). The effective thickness of a standard 2DEG in a quantum well or hetero structure is typically approximately 5-50 nm [173]. Due to construction constraints and the fact that confined electron wave functions have an evanescent tail that spreads through the barriers, this is the case. Graphene on the other side is only a single layer of carbon atoms, generally regarded to have a thickness of about 3 Å (twice the carbon-carbon bond length) [23].

Theoretical studies on the structure of 2D boron: Boron atoms may easily make chemical bonds due to the lack of electrons in the outermost layer. As a result, boron is chemically active and creates compounds with a diversity of crystal shapes. The fundamental crystal structure of bulk boron (Fig. 8) is based on a B12 icosahedron as the basic structural unit, with several forms of boron crystals being created on the B12 icosahedron using various connections and bonding processes [40]. As a result, unlike graphene, the boron block is not a layered structure, making borophene synthesis complex and difficult. Although borophene theoretical research has yielded promising results in recent years, boron synthesis methods and applications remain limited [174]. The first synthesis of borophene was achieved in 2015 in the laboratory [36].

A novel boron single layer structure, α-sheet, consisting of triangular lattice and hexagonal honeycomb holes, was predicted; afterwards, by computation, a novel boron single layer structure, α-sheet, was found [175]. Boron atoms in the -sheet are in the same plane, with lower energy than the buckling triangular form, which was previously thought to be the most stable. Based on this, between 2007 and 2014, a variety of classical borophene structures such as β-sheet, snub-sheet, α1-sheet, struc-1/8-sheet, β1-sheet, *Pmmn*-sheet, *Pmmm*-sheet were created by arranging hexagonal and triangular lattices in different ways [176]. These structures have a very low and nearly equal energy.

Borophene has a variety of structures, classified according to the composition patterns: (i) distorted hexagonal (DH) plane; (ii) buckled triangular (BT) plane; and (iii) mixed triangular-hexagonal (MTH) plane or to coordination number (CN)–α type (CN = 5, 6), β type (CN = 4, 5, 6), χ type (CN = 4, 5), δ

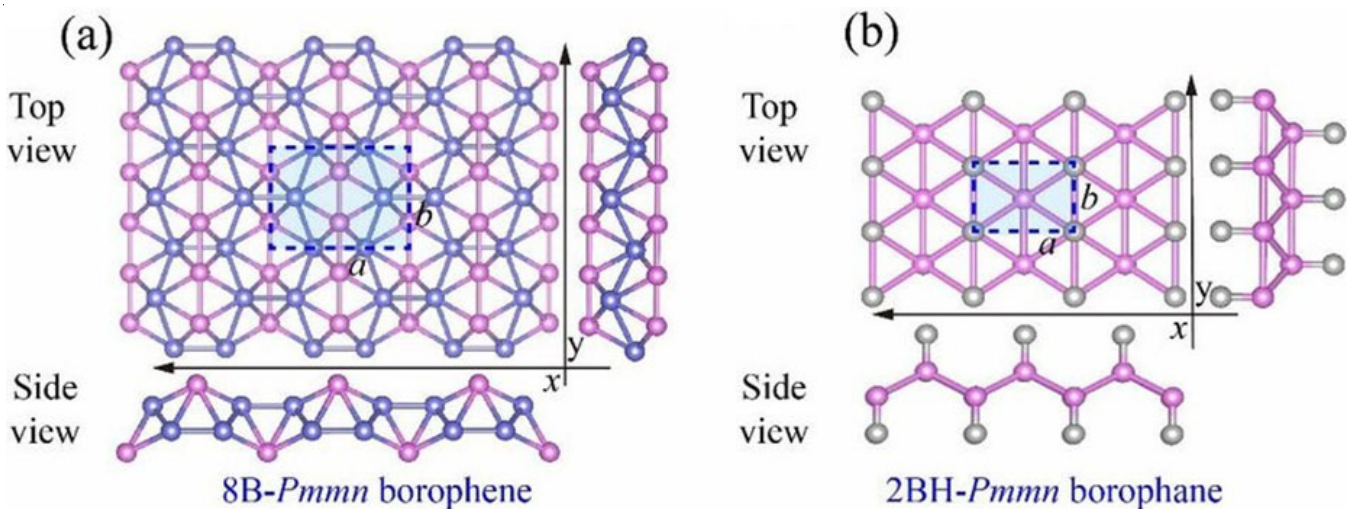

Fig. 8. Crystal structure of borophene (a) 8 B-Pmmn borophene (b) 2 BH-*P*mmn borophane

type (CN = m, m is a single number) and ψ type (CN = 3, 4, 5) [43]. Combining the two classifications, one can find that both the DH plane and the BT plane belong to the δ type plane and the MTH plane includes all planes except the δ type.

However, because borophene has multiple hexagonal hole arrangements, it is impractical to predict every conceivable structure using the density functional theory (DFT) technique alone. Borophene was considered as a pseudo-alloy by Yakobson *et al.* [11]. They also discovered that when hexagonal holes concentrations are in between 10% and 15%, borophene is highly stable and the cohesive energies of borophene with different structures are extremely low and near in the limited range of hexagonal holes concentrations previously described.

Challenges for the further applications of borophene: For future borophene uses, large-scale manufacture of quality controlled borophene remains a serious problem. The bottom-up and top-down techniques both have drawbacks. The CDV and PVD are two traditional bottom-up processes for borophene production, however they are harsh, expensive and generate materials with a small surface area (larger surface area of borophene is more suitable for further application on electronic equipment). Furthermore, borophene transfer from the metal substrate is problematic and environmental contamination is a possibility, both of which make subsequent uses in electrical devices more difficult. Although the top-down process is more cost-effective and easier, the thickness of borophene is not consistent and achieving a single-layer atomic thickness is challenging. As a result, creating an effective technique of synthesizing controllable-quality borophene will aid in the advancement of borophene's use and development.

Conclusion

Borophene possesses a number of intriguing features, including light weight, exceptional mechanical toughness, great superconducting capabilities and a number of remarkable biological qualities, all of which increase its application potential in electrical equipments and biomedicines. The evolution of the theoretical structure of borophene, as well as the borophene synthesis techniques and the variables impacting these, were reported and studied in depth in this review article. In this review article, the development of experimental borophene (2D material) synthesis has been the centre of interest. One of the most intriguing topics in materials research nowadays is the creation of 2D materials. Just over a decade, after the synthesis of graphene, the computationally guided synthesis of borophene can be regarded a roadmap for the production of novel 2D materials. Significant technological obstacles remain in borophene development, including as scaling up production methods, but its extraordinary and unique properties are projected to open up new possibilities in flexible electronics, battery and sensor technologies.

CONFLICT OF INTEREST

The authors declare that there is no conflict of interests regarding the publication of this article.

REFERENCES

1. M. Hempel, D. Nezich, J. Kong and M. Hofmann, *Nano Lett.*, **12**, 5714 (2012); https://doi.org/10.1021/nl302959a
2. M.I. Katsnelson, *Mater. Today*, **10**, 20 (2007); https://doi.org/10.1016/S1369-7021(06)71788-6
3. A.H. Castro Neto, F. Guinea, N.M.R. Peres, K.S. Novoselov and A.K. Geim, *Rev. Mod. Phys.*, **81**, 109 (2009); https://doi.org/10.1103/RevModPhys.81.109
4. A.K. Geim and K.S. Novoselov, *Nat. Mater.*, **6**, 183 (2007); https://doi.org/10.1038/nmat1849
5. D. Li and R.B. Kaner, *Science*, **320**, 1170 (2008); https://doi.org/10.1126/science.1158180
6. A.K. Geim, *Science*, **324**, 1530 (2009); https://doi.org/10.1126/science.1158877
7. T. Fan, Z. Xie, W. Huang, Z. Li and H. Zhang, *Nanotechnology*, **30**, 114002 (2019); https://doi.org/10.1088/1361-6528/aafc0f
8. Z. Xie, Y.P. Peng, L. Yu, C. Xing, M. Qiu, J. Hu and H. Zhang, *Solar RRL*, **4**, 1900400 (2020); https://doi.org/10.1002/solr.201900400
9. Y. Zhou, M. Zhang, Z. Guo, L. Miao, S.-T. Han, Z. Wang, X. Zhang, H. Zhang and Z. Peng, *Mater. Horiz.*, **4**, 997 (2017); https://doi.org/10.1039/C7MH00543A
10. L. Shahriary and A. Athawale, *Int. J. Renew. Energy Environ. Eng.*, **2**, 57 (2014).

11. A.J. Mannix, Z. Zhang, N.P. Guisinger, B.I. Yakobson and M.C. Hersam, *Nat. Nanotechnol.*, **13**, 444 (2018); https://doi.org/10.1038/s41565-018-0157-4
12. Z. Xie, C. Xing, W. Huang, T. Fan, Z. Li, J. Zhao, Y. Xiang, Z. Guo, J. Li, Z. Yang, B. Dong, J. Qu, D. Fan and H. Zhang, *Adv. Funct. Mater.*, **28**, 1705833 (2018); https://doi.org/10.1002/adfm.201705833
13. Z.-Q. Wang, T.-Y. Lü, H.-Q. Wang, Y.P. Feng and J.-C. Zheng, *Front. Phys.*, **14**, 33403 (2019); https://doi.org/10.1007/s11467-019-0884-5
14. Z. Xie, Y. Duo, Z. Lin, T. Fan, C. Xing, L. Yu, R. Wang, M. Qiu, Y. Zhang, Y. Zhao, X. Yan and H. Zhang, *Adv. Sci.*, **7**, 1902236 (2020); https://doi.org/10.1002/advs.201902236
15. P. Li, Y. Chen, T. Yang, Z. Wang, H. Lin, Y. Xu, L. Li, H. Mu, B.N. Shivananju, Y. Zhang, Q. Zhang, A. Pan, S. Li, D. Tang, B. Jia, H. Zhang and Q. Bao, *ACS Appl. Mater. Interfaces*, **9**, 12759 (2017); https://doi.org/10.1021/acsami.7b01709
16. J. Kwon and J. Kim, *Mater. Express*, **8**, 299 (2018); https://doi.org/10.1166/mex.2018.1430
17. Z. Zhang, E.S. Penev and B.I. Yakobson, *Chem. Soc. Rev.*, **46**, 6746 (2017); https://doi.org/10.1039/C7CS00261K
18. C. Xing, W. Huang, Z. Xie, J. Zhao, D. Ma, T. Fan, W. Liang, Y. Ge, B. Dong, J. Li and H. Zhang, *ACS Photonics*, **5**, 621 (2018); https://doi.org/10.1021/acsphotonics.7b01211
19. J. Chen, T. Fan, Z. Xie, Q. Zeng, P. Xue, T. Zheng, Y. Chen, X. Luo and H. Zhang, *Biomaterials*, **237**, 119827 (2020); https://doi.org/10.1016/j.biomaterials.2020.119827
20. S.-Y. Xie, Y. Wang and X.-B. Li, *Adv. Mater.*, **31**, 1900392 (2019); https://doi.org/10.1002/adma.201900392
21. W. Yi, W. Liu, J. Botana, L. Zhao, Z. Liu, J. Liu and M. Miao, *J. Phys. Chem. Lett.*, **8**, 2647 (2017); https://doi.org/10.1021/acs.jpclett.7b00891
22. J. Yu, M. Zhou, M. Yang, Q. Yang, Z. Zhang and Y. Zhang, *ACS Appl. Energy Mater.*, **3**, 11699 (2020); https://doi.org/10.1021/acsaem.0c01808
23. D.R. Cooper, B. D'Anjou, N. Ghattamaneni, B. Harack, M. Hilke, A. Horth, N. Majlis, M. Massicotte, L. Vandsburger, E. Whiteway and V. Yu, *Conden. Matter Phys.*, **2012**, 501686 (2011); https://doi.org/10.5402/2012/501686
24. Y. Zhao, S. Zeng and J. Ni, *Phys. Rev. B*, **93**, 014502 (2016); https://doi.org/10.1103/PhysRevB.93.014502
25. S.H. Mir, S. Chakraborty, P.C. Jha, J. Wärnå, H. Soni, P.K. Jha and R. Ahuja, *Appl. Phys. Lett.*, **109**, 053903 (2016); https://doi.org/10.1063/1.4960102
26. X. Tan, H.A. Tahini and S.C. Smith, *ACS Appl. Mater. Interfaces*, **9**, 19825 (2017); https://doi.org/10.1021/acsami.7b03676
27. Q. Sun, Z. Li, D.J. Searles, Y. Chen, G.M. Lu and A. Du, *J. Am. Chem. Soc.*, **135**, 8246 (2013); https://doi.org/10.1021/ja400243r
28. Y.W. Chen-Yang, H.C. Yang, G.J. Li and Y.K. Li, *J. Polym. Res.*, **11**, 275 (2005); https://doi.org/10.1007/s10965-005-3982-8
29. R. Peköz, M. Konuk, M.E. Kilic and E. Durgun, *ACS Omega*, **3**, 1815 (2018); https://doi.org/10.1021/acsomega.7b01730
30. D. Li, J. He, G. Ding, Q.Q. Tang, Y. Ying, J. He, C. Zhong, Y. Liu, C. Feng, Q. Sun, H. Zhou, P. Zhou and G. Zhang, *Adv. Funct. Mater.*, **28**, 1801685 (2018); https://doi.org/10.1002/adfm.201801685
31. A.N. Kolmogorov and S. Curtarolo, *Phys. Rev. B Condens. Matter Mater. Phys.*, **73**, 180501 (2006); https://doi.org/10.1103/PhysRevB.73.180501
32. S. Xu, Y. Zhao, J. Liao, X. Yang and H. Xu, *Nano Res.*, **9**, 2616 (2016); https://doi.org/10.1007/s12274-016-1148-0
33. D. Cohen-Tanugi and J.C. Grossman, *Nano Lett.*, **12**, 3602 (2012); https://doi.org/10.1021/nl3012853
34. M. Amjadi, A. Pichitpajongkit, S. Lee, S. Ryu and I. Park, *ACS Nano*, **8**, 5154 (2014); https://doi.org/10.1021/nn501204t
35. S. Chevalier, G. Caboche, K. Przybylski, and T. Brylewski, *J. Appl. Electrochem.*, **39**, 529 (2009); https://doi.org/10.1007/s10800-008-9726-9
36. A.J. Mannix, X.F. Zhou, B. Kiraly, J.D. Wood, D. Alducin, B.D. Myers, X. Liu, B.L. Fisher, U. Santiago, J.R. Guest, M.J. Yacaman, A. Ponce, A.R. Oganov, M.C. Hersam and N.P. Guisinger, *Science*, **350**, 1513 (2015); https://doi.org/10.1126/science.aad1080
37. G. Sachdeva, S. Kaur, R. Pandey and S.P. Karna, *Computation*, **9**, 101 (2021); https://doi.org/10.3390/computation9090101
38. A. Rastgou, H. Soleymanabadi and A. Bodaghi, *Microelectron. Eng.*, **169**, 9 (2017); https://doi.org/10.1016/j.mee.2016.11.012
39. A. Lherbier, A.R. Botello-Méndez and J.-C. Charlier, *2D Materials*, **3**, 045006 (2016); https://doi.org/10.1088/2053-1583/3/4/045006
40. H. Zhong, K. Huang, G. Yu and S. Yuan, *Phys. Rev. B*, **98**, 054104 (2018); https://doi.org/10.1103/PhysRevB.98.054104
41. B. Peng, H. Zhang, H. Shao, Y. Xu, R. Zhang and H. Zhu, *J. Mater. Chem. C Mater. Opt. Electron. Devices*, **4**, 3592 (2016); https://doi.org/10.1039/C6TC00115G
42. S.-H. Shin, Y.-H. Kim, M.H. Lee, J.-Y. Jung and J. Nah, *ACS Nano*, **8**, 2766 (2014); https://doi.org/10.1021/nn406481k
43. V. Bhavanasi, V. Kumar, K. Parida, J. Wang and P. S. Lee, *ACS Appl. Mater. Interfaces*, **8**, 521 (2016); https://doi.org/10.1021/acsami.5b09502
44. A. Yar and A. Ilyas, *J. Phys. Soc. Jpn.*, **89**, 124705 (2020); https://doi.org/10.7566/JPSJ.89.124705
45. T.P. Cysne, F.S.M. Guimarães, L.M. Canonico, T.G. Rappoport and R.B. Muniz, *Phys. Rev. B*, **104**, (2021); https://doi.org/10.1103/PhysRevB.104.165403
46. E.S. Penev, A. Kutana and B.I. Yakobson, *Nano Lett.*, **16**, 2522 (2016); https://doi.org/10.1021/acs.nanolett.6b00070
47. P. Gannon, C.T. Tripp, A.K. Knospe, C.V.Ramana, M. Deibert, R.J. Smith, V.I. Gorokhovsky, V. Shutthanandan and D. Gelles, *Surf. Coat. Technol.*, **188-189**, 55 (2004); https://doi.org/10.1016/j.surfcoat.2004.08.067
48. J.H. Liao, Y.C. Zhao, Y.J. Zhao, H. Xu and X.B. Yang, *Phys. Chem. Chem. Phys.*, **19**, 29237 (2017); https://doi.org/10.1039/C7CP06180C
49. K.S. Novoselov, A.K. Geim, S.V. Morozov, D. Jiang, M.I. Katsnelson, I.V. Grigorieva, S.V. Dubonos and A.A. Firsov, *Nature*, **438**, 197 (2005); https://doi.org/10.1038/nature04233
50. J. Nong, X. Xiao, F. Feng, B. Zhao, C. Min, X. Yuan and M. Somekh, *Optics Exp.*, **29**, 27750 (2021); https://doi.org/10.1364/OE.432844
51. H. Gonzalez-Herrero, J.M. Gomez-Rodriguez, P. Mallet, M. Moaied, J.J. Palacios, C. Salgado, M.M. Ugeda, J.-Y. Veuillen, F. Yndurain and I. Brihuega, *Science*, **352**, 437 (2016); https://doi.org/10.1126/science.aad8038
52. M. Ezawa, *Phys. Rev. B*, **96**, 035425 (2017); https://doi.org/10.1103/PhysRevB.96.035425
53. Y.-Q. Wang, T. Morimoto and J.E. Moore, *Phys. Rev. B*, **101**, 174419 (2020); https://doi.org/10.1103/PhysRevB.101.174419
54. G. Chang, S.-Y. Xu, B.J. Wieder, D.S. Sanchez, S.-M. Huang, I. Belopolski, T.-R. Chang, S. Zhang, A. Bansil, H. Lin and M.Z. Hasan, *Phys. Rev. Lett.*, **119**, 206401 (2017); https://doi.org/10.1103/PhysRevLett.119.206401
55. S. Saxena and A.K. Srivastava, *AIP Conf. Proc.*, **2369**, 020008 (2021); https://doi.org/10.1063/5.0061174
56. S. Saxena and A.K. Srivastava, *AIP Conf. Proc.*, **2220**, 140043 (2020), https://doi.org/10.1063/5.0001188
57. S. Sheng, J.B. Wu, X. Cong, Q. Zhong, W. Li, W. Hu, J. Gou, P. Cheng, P.-H. Tan, L. Chen and K. Wu, *ACS Nano*, **13**, 4133 (2019); https://doi.org/10.1021/acsnano.8b08909
58. N.T. Tien, T.Q. Trung, Y.G. Seoul, D.I. Kim and N.-E. Lee, *ACS Nano*, **5**, 7069 (2011); https://doi.org/10.1021/nn2017827
59. L.M. Canonico, T.P. Cysne, A. Molina-Sanchez, R.B. Muniz and T.G. Rappoport, *Phys. Rev. B*, **101**, (2020); https://doi.org/10.1103/PhysRevB.101.161409
60. S.I. Vishkayi and M.B. Tagani, *Phys. Chem. Chem. Phys.*, **20**, 10493 (2018); https://doi.org/10.1039/C7CP08671G

61. I. Boustani, A. Quandt, E. Hernandez and A. Rubio, *J. Chem. Phys.*, **110**, 3176 (1999); https://doi.org/10.1063/1.477976
62. M. Evans, J. Joannopoulos and S. Pantelides, *Phys. Rev. B Condens. Matter Mater. Phys.*, **72**, 045434 (2005); https://doi.org/10.1103/PhysRevB.72.045434
63. I. Boustani, A. Rubio and J.A. Alonso, *Surf. Sci.*, **370**, 355 (1997); https://doi.org/10.1016/S0039-6028(96)00969-7
64. B. Feng, O. Sugino, R.-Y. Liu, J. Zhang, R. Yukawa, M. Kawamura, T. Iimori, H. Kim, Y. Hasegawa, H. Li, L. Chen, K. Wu, H. Kumigashira, F. Komori, T.-C. Chiang, S. Meng and I. Matsuda, *Phys. Rev. Lett.*, **118**, 096401 (2017); https://doi.org/10.1103/PhysRevLett.118.096401
65. Z. Meng, T.C. Lang, S. Wessel, F.F. Assaad and A. Muramatsu, *Nature*, **464**, 847 (2010); https://doi.org/10.1038/nature08942
66. Z.A. Piazza, H.-S. Hu, W.-L. Li, Y.-F. Zhao, J. Li and L.-S. Wang, *Nat. Commun.*, **5**, 3113 (2014); https://doi.org/10.1038/ncomms4113
67. R.A. Ng, A. Wild, M.E. Portnoi and R.R. Hartmann, *Sci. Rep.*, **12**, 7688 (2022); https://doi.org/10.1038/s41598-022-11742-3
68. C. Lian, S.-Q. Hu, J. Zhang, C. Cheng, Z. Yuan, S. Gao and S. Meng, *Phys. Rev. Lett.*, **125**, 116802 (2020); https://doi.org/10.48550/arXiv.1803.01604
69. S. Gupta, A. Kutana and B.I. Yakobson, *J. Phys. Chem. Lett.*, **9**, 2757 (2018); https://doi.org/10.1021/acs.jpclett.8b00640
70. F. Crasto de Lima, G. J. Ferreira, and R. H. Miwa, *Nano Lett.*, **19**, 6564 (2019); https://doi.org/10.1021/acs.nanolett.9b02802
71. M. Khosravi, M. Mansouri, A. Gholami and Y. Yaghoubinezhad, *Int. J. Miner. Metall. Mater.*, **27**, 505 (2020); https://doi.org/10.1007/s12613-020-1966-7
72. T. Zhang, J. Shen, L. Lü, C. Wang, J. Sang and D. Wu, *Trans. Nonferrous Met. Soc. China*, **27**, 1285 (2017); https://doi.org/10.1016/S1003-6326(17)60149-3
73. H. Jafarlou, K. Hassannezhad, H. Asgharzadeh and G. Marami, *Mater. Sci. Technol.*, **34**, 455 (2018); https://doi.org/10.1080/02670836.2017.1407543
74. S. Qi, X. Li and H. Dong, *Mater. Lett.*, **209**, 15 (2017); https://doi.org/10.1016/j.matlet.2017.07.087
75. H. Tang and S. Ismail-Beigi, *Phys. Rev. Lett.*, **99**, 115501 (2007); https://doi.org/10.1103/PhysRevLett.99.115501
76. M. Xiong, C. Fan, Z. Zhao, Q. Wang, J. He, D. Yu, Z. Liu, B. Xu and Y. Tian, *J. Mater. Chem. C*, **2**, 7022 (2014); https://doi.org/10.1039/C4TC00938J
77. E.S. Penev, S. Bhowmick, A. Sadrzadeh and B.I. Yakobson, *Nano Lett.*, **12**, 2441 (2012); https://doi.org/10.1021/nl3004754
78. J.E. Padilha, R. H. Miwa and A. Fazzio, *Phys. Chem. Chem. Phys.*, **18**, 25491 (2016); https://doi.org/10.1039/C6CP05092A
79. M. Yi and Z. Shen, *J. Mater. Chem. A Mater. Energy Sustain.*, **3**, 11700 (2015); https://doi.org/10.1039/C5TA00252D
80. F. Crasto de Lima, G.J. Ferreira and R.H. Miwa, *J. Chem. Phys.*, **150**, 234701 (2019); https://doi.org/10.1063/1.5100679
81. A. Alexandradinata and B.A. Bernevig, *Phys. Scr.*, **164**, 014013 (2015); https://doi.org/10.1088/0031-8949/2015/T164/014013
82. G.J. Ferreira and D. Loss, *Phys. Rev. Lett.*, **111**, 106802 (2013); https://doi.org/10.1103/PhysRevLett.111.106802
83. J.-C. Rojas-S'anchez, S. Oyarz'un, Y. Fu, A. Marty, C. Vergnaud, S. Gambarelli, L. Vila, M. Jamet, Y. Ohtsubo, A. Taleb-Ibrahimi, P. Le F'evre, F. Bertran, N. Reyren, J.-M. George and A. Fert, *Phys. Rev. Lett.*, **116**, 096602 (2016); https://doi.org/10.1103/PhysRevLett.116.096602
84. F.C. de Lima, G.J. Ferreira and R.H. Miwa, *Phys. Rev. B*, **96**, 115426 (2017); https://doi.org/10.1103/PhysRevB.96.115426
85. F.C. de Lima, G.J. Ferreira and R.H. Miwa, *Phys. Chem. Chem. Phys.*, **21**, 22344 (2019); https://doi.org/10.1039/C9CP04760C
86. G. Chang, B.J. Wieder, F. Schindler, D.S. Sanchez, I. Belopolski, S.-M. Huang, B. Singh, D. Wu, T.-R. Chang, T. Neupert, S.-Y. Xu, H. Lin and M.Z. Hasan, *Nat. Mater.*, **17**, 978 (2018); https://doi.org/10.1038/s41563-018-0169-3
87. P. Xiang, X. Chen, W. Zhang, J. Li, B. Xiao, L. Li and K. Deng, *Phys. Chem. Chem. Phys.*, **19**, 24945 (2017); https://doi.org/10.1039/C7CP04989G
88. S. Das, D. Lahiri, D.-Y. Lee, A. Agarwal and W. Choi, *Carbon*, **59**, 121 (2013); https://doi.org/10.1016/j.carbon.2013.02.063
89. X. Wu, J. Dai, Y. Zhao, Z. Zhuo, J. Yang and X.C. Zeng, *ACS Nano*, **6**, 7443 (2012); https://doi.org/10.1021/nn302696v
90. P. Canfield, D.K. Finnemore, S.L. Bud'ko, J.E. Ostenson, G. Lapertot, C.E. Cunningham and C. Petrovic, *Phys. Rev. Lett.*, **86**, 2423 (2001); https://doi.org/10.1103/PhysRevLett.86.2423
91. C. Cheng, J.T. Sun, H. Liu, H.-X. Fu, J. Zhang, X.-R. Chen and S. Meng, *2D Materials*, **4**, 025032 (2017); https://doi.org/10.1088/2053-1583/aa5e1b
92. Y.-P. Zhou and J.-W. Jiang, *Sci. Rep.*, **7**, 45516 (2017); https://doi.org/10.1038/srep45516
93. J. Yang, R. Quhe, S. Feng, Q. Zhang, M. Lei and J. Lu, *Phys. Chem. Chem. Phys.*, **19**, 23982 (2017); https://doi.org/10.1039/C7CP04570K
94. K. Pu, A.J. Shuhendler, J.V. Jokerst, J. Mei, S.S. Gambhir, Z. Bao and J. Rao, *Nat. Nanotechnol.*, **9**, 233 (2014); https://doi.org/10.1038/nnano.2013.302
95. B.H. Hong, *IEEE 69th Device Res. Conf.*, 37-38 (2011); https://doi.org/10.1109/DRC.2011.5994410
96. L. Kong, L. Liu, L. Chen, Q. Zhong, P. Cheng, H. Li, Z. Zhang and K. Wu, *Nanoscale*, **11**, 15605 (2019); https://doi.org/10.1039/C9NR03792F
97. Z.-Y. Xie, L.-G. Sun, G.-Z. Han and Z.-Z. Gu, *Adv. Mater.*, **20**, 3601 (2008); https://doi.org/10.1002/adma.200800495
98. G. Tai, T. Hu, Y. Zhou, X. Wang, J. Kong, T. Zeng, Y. You and Q. Wang, *Angew. Chem. Int. Ed.*, **54**, 15473 (2015); https://doi.org/10.1002/anie.201509285
99. K.S. Novoselov, A.K. Geim, S.V. Morozov, D. Jiang, Y. Zhang, S.V. Dubonos, I.V. Grigorieva and A.A. Firsov, *Science*, **306**, 666 (2004); https://doi.org/10.1126/science.1102896
100. S. Bae, H. Kim, Y. Lee, X. Xu, J.-S. Park, Y. Zheng, J. Balakrishnan, T. Lei, H.R. Kim, Y.I. Song, Y.-J. Kim, K.S. Kim, B. Ozyilmaz, J.-H. Ahn, B.H. Hong and S. Iijima, *Nat. Nanotechnol.*, **5**, 574 (2010); https://doi.org/10.1038/nnano.2010.132
101. Y. Yu, C. Li, Y. Liu, L. Su, Y. Zhang and L. Cao, *Sci. Rep.*, **3**, 1866 (2013); https://doi.org/10.1038/srep01866
102. M. Kandpal, V. Palaparthy, N. Tiwary and V.R. Rao, *IEEE Trans. NanoTechnol.*, **16**, 259 (2017); https://doi.org/10.1109/TNANO.2017.2659383
103. K.-S. Kim, H.-J. Lee, C. Lee, S.-K. Lee, H. Jang, J.-H. Ahn, J.-H. Kim and H.-J. Lee, *ACS Nano*, **5**, 5107 (2011); https://doi.org/10.1021/nn2011865
104. X. Wang, H. You, F. Liu, M. Li, L. Wan, S. Li, Q. Li, Y. Xu, R. Tian, Z. Yu, D. Xiang and J. Cheng, *Chem. Vap. Depos.*, **15**, 53 (2009); https://doi.org/10.1002/cvde.200806737
105. A. Nag, K. Raidongia, K.P.S.S. Hembram, R. Datta, U.V. Waghmare and C.N.R. Rao, *ACS Nano*, **4**, 1539 (2010); https://doi.org/10.1021/nn9018762
106. V.B. Mbayachi, E. Ndayiragije, T. Sammani, S. Taj, E.R. Mbuta and A.U. Khan, *Results Chem.*, **3**, 100163 (2021); https://doi.org/10.1016/j.rechem.2021.100163
107. W. Choi, I. Lahiri, R. Seelaboyina and Y.S. Kang, *Crit. Rev. Solid State Mater. Sci.*, **35**, 52 (2010); https://doi.org/10.1080/10408430903505036

108. X. Li, W. Cai J. An, S. Kim, J. Nah, D. Yang, A. Velamakanni, R. Piner, I. Jung, E. Tutuc, S.K. Banerjee, L. Colombo and R.S. Ruoff, *Science*, **324**, 1312 (2009); https://doi.org/10.1126/science.1171245
109. S. Stankovich, D.A. Dikin, R.D. Piner, K.A. Kohlhaas, A. Kleinhammes, Y. Jia, Y. Wu, S.B.T. Nguyen and R.S. Ruoff, *Carbon*, 45, 1558 (2007); https://doi.org/10.1016/j.carbon.2007.02.034
110. X.W. Fu, Z.-M. Liao, J.-X. Zhou, Y.-B. Zhou, H.-C. Wu, R. Zhang, G. Jing, J. Xu, X. Wu, W. Guo and D. Yu, *Appl. Phys. Lett*., **99**, 213107 (2011); https://doi.org/10.1063/1.3663969
111. K. Tripathi, G. Gyawali and S.W. Lee, *ACS Appl. Mater. Interfaces*, **9**, 32336 (2017); https://doi.org/10.1021/acsami.7b07922
112. H. Duan, E. Xie, L. Han and Z. Xu, *Adv. Mater.*, **20**, 3284 (2008); https://doi.org/10.1002/adma.200702149
113. M.J. Allen, V.C. Tung and R. Kaner, *Chem. Rev*., **110**, 132 (2010); https://doi.org/10.1021/cr900070d
114. J. Li, X. Zeng, T. Ren and E.V. der Heide, *Lubricants*, **2**, 137 (2014); https://doi.org/10.3390/lubricants2030137
115. J. Ou, J. Wang, S. Liu, B. Mu, J. Ren, H. Wang and S. Yang, *Langmuir*, **26**, 15830 (2010); https://doi.org/10.1021/la102862d
116. S. Qi, X. Li and H. Dong, *Mater. Lett.*, **209**, 15 (2017); https://doi.org/10.1016/j.matlet.2017.07.087
117. L. Wu, Alamusi, J. Xue, T. Itoi, N. Hu, Y. Li, C. Yan, J. Qiu, H. Ning, W. Yuan and B. Gu, *J. Intell. Mater. Syst. Struct.*, **25**, 1813 (2014); https://doi.org/10.1177/1045389X14529609
118. J. Mondal, M. Marandi, J. Kozlova, M. Merisalu, A. Niilisk and V. Sammelselg, *J. Chem. Chem. Eng.*, **8**, 786 (2014).
119. S. Yi, G. Li, S. Ding, J. Mo and M. Rahman, Experimental Study of Graphene Oxide Suspension in Drilling Ti-6Al-4V; In: Proceedings of the 2nd Information Technology and Mechatronics Engineering Conference (ITOEC 2016), Atlantis Press (2016).
120. Z. Xie, X. Meng, X. Li, W. Liang, W. Huang, K. Chen, J. Chen, C. Xing, M. Qiu, B. Zhang, G. Nie, N. Xie, X. Yan and H. Zhang, *Research*, **2020**, Article ID 2624617 (2020); https://doi.org/10.34133/2020/2624617
121. S. Luo and T. Liu, *Adv. Mater.*, **25**, 5650 (2013); https://doi.org/10.1002/adma.201301796
122. M. Fattahi, A.R. Gholami, A. Eynalvandpour, E. Ahmadi, Y. Fattahi and S. Akhavan, *Micron*, **64**, 20 (2014); https://doi.org/10.1016/j.micron.2014.03.013
123. M. Yang, H. Jin, Z. Sun and R. Gui, *J. Mater. Chem. A*, **10**, 5111 (2022); https://doi.org/10.1039/D1TA10132C
124. L. Zhu, B. Zhao, T. Zhang, G. Chen and S.A. Yang, *J. Phys. Chem. C*, **123**, 14858 (2019); https://doi.org/10.1021/acs.jpcc.9b03447
125. B. Kiraly, X. Liu, L. Wang, Z. Zhang, A.J. Mannix, B.L. Fisher, B.I. Yakobson, M.C. Hersam and N.P. Guisinger, *ACS Nano*, **13**, 3816 (2019); https://doi.org/10.1021/acsnano.8b09339
126. H. Liu, J. Gao and J. Zhao, *Sci. Rep.*, **3**, 3238 (2013); https://doi.org/10.1038/srep03238
127. G. Bhattacharyya, A. Mahata, I. Choudhuri and B. Pathak, *J. Phys. D Appl. Phys.*, **50**, 405103 (2017); https://doi.org/10.1088/1361-6463/aa81b8
128. H.R. Jiang, Z. Lu, M.C. Wu, F. Ciucci and T.S. Zhao, *Nano Energy*, **23**, 97 (2016); https://doi.org/10.1016/j.nanoen.2016.03.013
129. R. Wu, I.K. Drozdov, S. Eltinge, P. Zahl, S. Ismail-Beigi, I. Bozovic and A. Gozar, *Nat. Nanotechnol.*, **14**, 44 (2019); https://doi.org/10.1038/s41565-018-0317-6
130. L. Kong, K. Wu and L. Chen, *Front. Phys.*, **13**, 138105 (2018); https://doi.org/10.1007/s11467-018-0752-8
131. B. Grunbaum and G.C. Shephard, *Math. Mag.*, **50**, 227 (1977); https://doi.org/10.1080/0025570X.1977.11976655
132. P. Ranjan, J.M. Lee, P. Kumar and A. Vinu, *Adv. Mater.*, **32**, 2000531 (2020); https://doi.org/10.1002/adma.202000531
133. W. Li, L. Kong, C. Chen, J. Gou, S. Sheng, W. Zhang, H. Li, L. Chen, P. Cheng and K. Wu, *Sci. Bull. (Beijing)*, **63**, 282 (2018); https://doi.org/10.1016/j.scib.2018.02.006
134. B. Feng, J. Zhang, Q. Zhong, W. Li, S. Li, H. Li, P. Cheng, S. Meng, L. Chen and K. Wu, *Nat. Chem.*, **8**, 563 (2016); https://doi.org/10.1038/nchem.2491
135. M. Novotný, F.J. Domínguez-Gutiérrez and P. Krstic, *J. Mater. Chem. C Mater. Opt. Electron. Devices*, **5**, 5426 (2017); https://doi.org/10.1039/C7TC00976C
136. S. Banerjee, G. Periyasamy and S.K. Pati, *J. Mater. Chem. A Mater. Energy Sustain.*, **2**, 3856 (2014); https://doi.org/10.1039/c3ta14041e
137. Y. Duo, Z. Xie, L. Wang, N.M. Abbasi, T. Yang, Z. Li, G. Hu and H. Zhang, *Coord. Chem. Rev*., **427**, 213549 (2021); https://doi.org/10.1016/j.ccr.2020.213549
138. D. Golberg, Y. Bando, Y. Huang, T. Terao, M. Mitome, C. Tang and C. Zhi, *ACS Nano*, **4**, 2979 (2010); https://doi.org/10.1021/nn1006495
139. C. Ataca, A. Ethem and S. Ciraci, *Phys. Rev. B*, **79**, 041406 (2009); https://doi.org/10.1103/PhysRevB.79.041406
140. X. Ji, N. Kong, J. Wang, W. Li, Y. Xiao, S.T. Gan, Y. Zhang, Y. Li, X. Song, Q. Xiong, S. Shi, Z. Li, W. Tao, H. Zhang, L. Mei and J. Shi, *Adv. Mater.*, **30**, 1803031 (2018); https://doi.org/10.1002/adma.201803031
141. Y. Liu, E.S. Penev and B.I. Yakobson, *Angew. Chem. Int. Ed.*, **52**, 3156 (2013); https://doi.org/10.1002/anie.201207972
142. L. Shi, T. Zhao, A. Xu and J. Xu, *Sci. Bull.*, **61**, 1138 (2016); https://doi.org/10.1007/s11434-016-1118-7
143. X. Li, M.M. Honari, Y. Fu, A. Kumar, H. Saghlatoon, P. Mousavi and H.-J. Chung, *Flex. Print. Electron*., **2**, 035001 (2017); https://doi.org/10.1088/2058-8585/aa73c9
144. J.Z. Gul, M. Sajid and K.H. Choi, *J. Mater. Chem. C Mater. Opt. Electron. Devices*, **7**, 4692 (2019); https://doi.org/10.1039/C8TC03423K
145. P. Cataldi, A. Athanassiou and S.I. Bayer, *Appl. Sci.*, **8**, 1438 (2018); https://doi.org/10.3390/app8091438
146. S. Bae, S.J. Kim, D. Shin, J.-H. Ahn and B.H. Hong, *Phys. Scr*., **2012**, 014024 (2012); https://doi.org/10.1088/0031-8949/2012/T146/014024
147. H. Rashtchi, M.A.F. Sani and A.M. Dayaghi, *Ceram. Int.*, **39**, 8123 (2013); https://doi.org/10.1016/j.ceramint.2013.03.085
148. M. Tatullo, B. Zavan, F. Genovese, B. Codispoti, I. Makeeva, S. Rengo, L. Fortunato and G. Spagnuolo, *Appl. Sci.*, **9**, 3446 (2019); https://doi.org/10.3390/app9173446
149. B.S. Tong and Y.M. Song, *Austin J. Nanomed. Nanotechnol.*, **3**, 1041 (2015).
139. X. Zhang, J. Hu, Y. Cheng, H.Y. Yang, Y. Yao and S.A. Yang, *Nanoscale*, **8**, 15340 (2016); https://doi.org/10.1039/C6NR04186H
140. D. Ma, Y. Li, H. Mi, S. Luo, P. Zhang, Z. Lin, J. Li and H. Zhang, *Angew. Chem. Int. Ed.*, **57**, 8901 (2018); https://doi.org/10.1002/anie.201802672
141. Q.-F. Li, C.G. Duan, X.G. Wan and J.L. Kuo, *J. Phys. Chem. C*, **119**, 8662 (2015); https://doi.org/10.1021/jp512411g
142. J. Liu, C. Zhang, L. Xu and S. Ju, *RSC Adv.*, **8**, 17773 (2018); https://doi.org/10.1039/C8RA01942H
143. L.V. Wang and S. Hu, *Science*, **335**, 1458 (2012); https://doi.org/10.1126/science.1216210
144. X. Liu, L. Wang, S. Li, M.S. Rahn, B.I. Yakobson and M.C. Hersam, *Nat. Commun.*, **10**, 1642 (2019); https://doi.org/10.1038/s41467-019-09686-w
145. X. Zhen, J. Zhang, J. Huang, C. Xie, Q. Miao and K. Pu, *Angew. Chem. Int. Ed.*, **57**, 7804 (2018); https://doi.org/10.1002/anie.201803321
146. B. Kang, D. Yu, Y. Dai, S. Chang, D. Chen and Y. Ding, *Small*, **5**, 1292 (2009); https://doi.org/10.1002/smll.200801820
147. B. Kang, Y. Dai, S. Chang and D. Chen, *Carbon*, **46**, 978 (2008); https://doi.org/10.1016/j.carbon.2008.03.004
148. D.Y. Lee, J.Y. Kim, Y. Lee, S. Lee, W. Miao, H.S. Kim, J.-J. Min and S. Jon, *Angew. Chem. Int. Ed.*, **56**, 13684 (2017); https://doi.org/10.1002/anie.201707137

149. Z. Sun, Y. Zhao, Z. Li, H. Cui, Y. Zhou, W. Li, W. Tao, H. Zhang, H. Wang, P.K. Chu and X.-F. Yu, *Small*, **13**, 1602896 (2017); https://doi.org/10.1002/smll.201602896
150. Z. Xie, S. Chen, Y. Duo, Y. Zhu, T. Fan, Q. Zou, M. Qu, Z. Lin, J. Zhao, Y. Li, L. Liu, S. Bao, H. Chen, D. Fan and H. Zhang, *ACS Appl. Mater. Interfaces*, **11**, 22129 (2019); https://doi.org/10.1021/acsami.9b04628
151. J. Li, W. Zhang, W. Ji, J. Wang, N. Wang, W. Wu, Q. Wu, X. Hou, W. Hu and L. Li, *J. Mater. Chem. B*, 9, 7909 (2021); https://doi.org/10.1039/D1TB01310F
152. H.S. Kim and Y.-H. Kim, *Biosens. Bioelectron.*, **69**, 186 (2015); https://doi.org/10.1016/j.bios.2015.02.020
153. S. Saxena and A.K. Srivastava, *AIP Conf. Proc*., **2220**, 020032 (2020); https://doi.org/10.1063/5.0001189
154. M. Donarelli and L. Ottaviano, *Sensors*, **18**, 3638 (2018); https://doi.org/10.3390/s18113638
155. L. Mahdavian, *J. Nanostructure Chem.*, **3**, 1 (2012); https://doi.org/10.1186/2193-8865-3-1
156. A.M. Attaran, S. Abdol-Manafi, M. Javanbakht and M. Enhessari, *J. Nanostruc. Chem.*, **6**, 121 (2016); https://doi.org/10.1007/s40097-015-0186-6
157. A.L. Verma, S. Saxena, G.S.S. Saini, V. Gaur and V.K. Jain, *Thin Solid Films*, **519**, 8144 (2011); https://doi.org/10.1016/j.tsf.2011.06.034
158. S. Saxena and A.L. Verma, *AIP Conf. Proc*., **1536**, 1298 (2013); https://doi.org/10.1063/1.4810718
159. S. Saxena and A.L. Verma, *Adv. Mater. Lett.*, **5**, 472 (2014); https://doi.org/10.5185/amlett.2013.2429
160. S. Saxena, G.S.S. Saini and A.L. Verma, *Bull. Mater. Sci.*, **38**, 443 (2015); https://doi.org/10.1007/s12034-015-0864-5
161. S. Saxena, A.K. Srivastava, R. Srivastava and V. Kheraj, *Eur. J. Eng. Sci. Tech.*, **2**, 70 (2019); https://doi.org/10.33422/EJEST.2019.08.18
162. A.M.L. Oliveira, M. Machado, G.A. Silva, D.B. Bitoque, J.T. Ferreira, L.A. Pinto and Q. Ferreira, *Nanomaterials*, **12**, 1149 (2022); https://doi.org/10.3390/nano12071149
163. K. Nedunchezhian, N. Aswath, M. Thiruppathy and S. Thirugnanamurthy, *J. Clin. Diagn. Res*., **10**, ZE01 (2016); https://doi.org/10.7860/JCDR/2016/19890.9024
164. A.K. Asbury, R.G. Ojeman, S.L. Nielsen and W.H. Sweet, *J. Neuropathol. Exp. Neurol.*, **31**, 278 (1972); https://doi.org/10.1097/00005072-197204000-00005
165. H. Hatanaka, Eds.: A.B.M.F. Karim and E.R. Laws, Boron Neutron Capture Therapy for Tumors In: Glioma, Springer, Berlin, Heidelberg (1986).
166. M. Ionita, G.M. Vlasceanu, A.A. Watzlawek, S.I. Voicu, J.S. Burns and H. Iovu, *Composit. B Eng*., **121**, 34 (2017); https://doi.org/10.1016/j.compositesb.2017.03.031
167. B. Kiraly, E.V. Iski, A.J. Mannix, B.L. Fisher, M.C. Hersam and N.P. Guisinger, *Nat. Nanotechnol*., **4**, 2804 (2013); https://doi.org/10.1038/ncomms3804
168. C.A. Castilla-Martinez, R. Moury, S. Ould-Amara and U.B. Demirci, *Energies*, **14**, 7003 (2021); https://doi.org/10.3390/en14217003
169. S.-Y. Xie, Y. Wang and X.-B. Li, *Adv. Mater.*, **31**, 1900392 (2019); https://doi.org/10.1002/adma.201900392
170. G. Qin, A. Du and Q. Sun, *Phys. Chem. Chem. Phys.*, **20**, 16216 (2018); https://doi.org/10.1039/C8CP01407H
171. L. Adamska, S. Sadasivam, J.J. Foley IV, P. Darancet and S. Sharifzadeh, *J. Phys. Chem. C*, **122**, 4037 (2018); https://doi.org/10.1021/acs.jpcc.7b10197
172. S.Z. Butler, S.M. Hollen, L. Cao, Y. Cui, J.A. Gupta, H.R. Gutiérrez, T.F. Heinz, S.S. Hong, J. Huang, A.F. Ismach, E. Johnston-Halperin, M. Kuno, V.V. Plashnitsa, R.D. Robinson, R.S. Ruoff, S. Salahuddin, J. Shan, L. Shi, M.G. Spencer, M. Terrones, W. Windl and J.E. Goldberger, *ACS Nano*, **7**, 2898 (2013); https://doi.org/10.1021/nn400280c
173. A.D. Bartolomeo, *Nanomaterials*, **10**, 579 (2020); https://doi.org/10.3390/nano10030579
174. P.T.T. Le, T.C. Phong and M. Yarmohammadi, *Phys. Chem. Chem. Phys.*, **21**, 21790 (2019); https://doi.org/10.1039/C9CP04719K
175. S.N. Shirodkar, E.S. Penev and B.I. Yakobson, *Sci. Bull.*, **63**, 270 (2018); https://doi.org/10.1016/j.scib.2018.02.019
176. J. Yuan, N. Yu, K. Xue and X. Miao, *RSC Adv*., **7**, 8654 (2017); https://doi.org/10.1039/C6RA28454J